



Past water flow beneath Pine Island and Thwaites glaciers, West Antarctica

5 James D. Kirkham^{1,2}, Kelly A. Hogan², Robert D. Larter², Neil S. Arnold¹, Frank O. Nitsche³,
Nicholas R. Golledge⁴, Julian A. Dowdeswell¹

¹Scott Polar Research Institute, University of Cambridge, Lensfield Road, Cambridge, CB2 1ER, UK.

²British Antarctic Survey, High Cross, Madingley Road, Cambridge CB3 0ET, UK.

10 ³Lamont-Doherty Earth Observatory of Columbia University, P.O. Box 1000, Palisades, NY 10964-8000 USA.

⁴Antarctic Research Centre, Victoria University of Wellington, Wellington 6140, New Zealand.

Correspondence to: jk675@cam.ac.uk

Abstract

15

Outburst floods from subglacial lakes beneath the Antarctic Ice Sheet modulate ice-flow velocities over periods of months to years. Although subglacial lake-drainage events have been observed from satellite-altimetric data, little is known about their role in the long-term evolution of ice-sheet basal hydrology. Here, we systematically map and model past water flow through an extensive area containing over 1000 subglacial channels and 19 former lake basins exposed on over 19,000 km² of seafloor by the retreat of Pine Island and Thwaites glaciers, West Antarctica. At 560 m wide and 50 m deep on average, the channels offshore of present-day Pine Island and Thwaites glaciers are approximately twice as deep, three times as wide, and cover an area over 400 times larger than the terrestrial meltwater channels comprising the Labyrinth in the Antarctic Dry Valleys. The channels incised into bedrock offshore of contemporary Pine Island and Thwaites glaciers would have been capable of accommodating discharges of up to $8.8 \times 10^6 \text{ m}^3 \text{ s}^{-1}$. We suggest that the channels were formed by episodic, high-magnitude discharges from subglacial lakes trapped during ice-sheet advance and retreat over multiple glacial periods. Our results document the widespread influence of episodic subglacial drainage events during past glacial periods, in particular beneath large ice streams similar to those that continue to dominate contemporary ice-sheet discharge.

30 1 Introduction

The widespread and accelerating retreat of Pine Island and Thwaites glaciers constitutes a potential threat to the stability of the West Antarctic Ice Sheet (WAIS) (Rignot *et al.*, 2008, 2014; Joughin *et al.*, 2014; Feldmann and Levermann, 2015; Shepherd *et al.*, 2018; Yu *et al.*, 2018). The routing, storage, and expulsion of subglacial water from beneath the WAIS directly influences its mass-loss rates and, accordingly, sea-level rise (Joughin *et al.*, 2002; Alley *et al.*, 2006; Bell *et al.*, 2007; Stearns *et al.*, 2008). Variability in subglacial water supply can lead to ice-sheet instability (Schoof, 2010). However, the effect of subglacial water as a lubricant at the basal ice-sheet boundary is still insufficiently understood to be accurately incorporated into the current generation of ice-sheet models, and is thus presently absent from assessments of future ice-sheet behaviour (Fricker and Scambos, 2009; Flowers, 2015; Fricker *et al.*, 2016).

40

Over recent decades, ice-penetrating radio-echo sounding surveys and satellite altimetry have revealed an intricate subglacial network of water storage and transfer beneath the contemporary Antarctic Ice Sheet. Over 400 ponded water bodies, termed subglacial lakes, have been detected beneath the ice (e.g. Robin *et al.*, 1970; Oswald and Robin, 1973; Siegert *et al.*, 1996, 2005, 2015), about a quarter of which have been observed to fill and drain over sub-decadal



45 timescales (Gray *et al.*, 2005; Wingham *et al.*, 2006; Fricker *et al.*, 2007; Smith *et al.*, 2009a, 2017). The subglacial
routing of the water released from this special class of ‘active’ subglacial lakes can be traced for hundreds of kilometres,
often triggering a cascade of further subglacial lake drainage downstream (Wingham *et al.*, 2006; Flament *et al.*, 2014;
Fricker *et al.*, 2007, 2014). In some instances, active lake drainage has been associated with temporary accelerations in
ice velocity (Stearns *et al.*, 2008). Active Antarctic subglacial lakes typically discharge relatively small volumes of water
50 over several months, with peak discharges of tens of cubic metres per second. For example, lakes detected in the
Adventure subglacial trench, East Antarctica, discharged 1.8 km³ of water over 16 months with a peak discharge of
~50 m³ s⁻¹ (Wingham *et al.*, 2006), whilst 3.7 km³ of water was released from a system of subglacial lakes beneath
Thwaites Glacier between June 2013 and January 2014 (Smith *et al.*, 2017). To date, the largest contemporary subglacial
lake drainage event observed in Antarctica was the loss of 5.2 ± 1.5 km³ of water from Lake Cook, East Antarctica, over
55 a 2-year period (Flament *et al.*, 2014).

Geomorphological evidence suggests that subglacial water movement, substantially larger than that documented
in the satellite era, has occurred beneath the Antarctic Ice Sheet in the past. The mountains flanking the Antarctic Dry
Valleys in southern Victoria Land and the ice-free margin of the East Antarctic Soya Coast contain abundant features
60 formed by the flow of subglacial meltwater (Denton *et al.*, 1984; Sawagaki and Hirakawa, 1997). Channel systems that
are kilometres long and hundreds of metres wide are present in the Asgard Range (Sugden *et al.*, 1991), in the foothills
of the Royal Society Range (Sugden *et al.*, 1999), and in the Convoy Range of the Transantarctic Mountains (Denton and
Sugden, 2005; Lewis *et al.*, 2006) (Fig. 1). One of the most spectacular relict Antarctic landscapes carved by subglacial
water is a 5-km long anastomosing system of terrestrial channels in Wright Valley termed the Labyrinth (Selby and
65 Wilson, 1971). The Labyrinth channels exceed 500 m in width and are incised over 150 m into a 300 m thick sill of Ferrar
Dolerite (Lewis *et al.*, 2006). Channel formation has been attributed to repeated subglacial outburst floods, with estimated
discharges of up to 1.6–2.2×10⁶ m³ s⁻¹, sourced from one or more subglacial lakes that became trapped as the Antarctic
Ice Sheet overrode the Transantarctic Mountains during the Miocene epoch (23–5.3 Ma BP) (Marchant *et al.*, 1993, 1996;
Denton and Sugden, 2005; Lewis *et al.*, 2006). The irregular reverse gradients, anastomosing structure, and the potholes
70 and plunge pools associated with the channel systems in southern Victoria Land are consistent with formation by
pressurised subglacial meltwater (Shreve, 1972; Marchant *et al.*, 2011) on a scale that is perhaps unequalled outside the
Channeled Scabland landscape of eastern Washington State — produced by some of the largest floods on Earth from
Pleistocene proglacial Lake Missoula (Bretz, 1923, 1969; Denton and Sugden, 2005; Evatt *et al.*, 2006).

75 Channels with similar dimensions have been identified submerged offshore on the largely bedrock-dominated
inner continental shelves of the western Antarctic Peninsula (e.g. Ó Cofaigh *et al.*, 2002, 2005; Domack *et al.*, 2006;
Anderson and Oakes-Fretwell, 2008), West Antarctica (e.g. Lowe and Anderson, 2002, 2003; Larter *et al.*, 2009; Nitsche
et al., 2013), and eroded into soft sediments in the inner Ross Sea (Simkins *et al.*, 2017). The observed landforms are
typically hundreds of metres wide, tens of metres deep, and possess undulating thalwegs that indicate incision by
80 pressurised subglacial meltwater (Lowe and Anderson, 2002). The size and widespread distribution of the offshore
channels implies that substantial quantities of subglacial meltwater were required for their formation; this inference is
fundamentally inconsistent with the quantity of meltwater produced at the Antarctic ice-bed interface currently (Nitsche
et al., 2013; Rose *et al.*, 2014) and the discharges associated with active subglacial lake water transfer (Wingham *et al.*,
2006; Stearns *et al.*, 2008). The physical process responsible for the formation of the large channel systems on the
85 Antarctic continental shelf thus remains unresolved, limiting our understanding of ice-sheet hydrology and future
ice-sheet behaviour.



90 In this study, we examine the origin and formation of a huge system of submarine channels, covering an area
>19,000 km² (over twice the size of Yellowstone National Park), located within 200 km of the present-day margins of
Pine Island and Thwaites glaciers. We map the detailed channel network and conduct a quantitative morphometric
comparison between the channels in Pine Island Bay and the terrestrial channels comprising the Labyrinth. We then use
a numerical model to simulate the subglacial hydrological conditions and water routing beneath Pine Island and Thwaites
glaciers during the Last Glacial Maximum (LGM), and provide constraints on the possible mechanisms and timescales
over which the submarine channels formed.

95 2 Methods

2.1 Bathymetric and terrestrial data

100 We used multibeam-bathymetric data, collected over two decades by extensive shipborne surveys in Pine Island
Bay, to produce a comprehensive high-resolution digital elevation model (DEM) of the seafloor offshore of modern Pine
Island and Thwaites glaciers (Table 1). The multibeam-bathymetric data were gridded at a 20-m resolution. A
conservative degree of interpolation, applied up to four cell widths away from a data-filled cell, was used to fill small
missing gaps in the grids when proximal to existing bathymetry data. This was the highest resolution that could be
achieved without requiring interpolation to fill more than 10 % of the study area's grid cells. In addition to the bathymetric
105 data, a 2-m horizontal resolution DEM of Wright Valley, in the McMurdo Dry Valleys of Antarctica, was obtained from
the National Aeronautics and Space Administration's 2001 Airborne Topographic Mapper laser altimetry survey to
examine the morphology of the Labyrinth (Schenk *et al.*, 2004).

2.2 Derivation of channel metrics

110 Channels were digitised manually using hill-shaded DEMs in ArcGIS 10.4. Comparison with a
three-dimensional representation of the study area, in which the digitised channel outlines were draped over the projected
DEM, ensured that the boundaries of the channels were demarcated accurately (Mayer *et al.*, 2000). This technique
permitted the routing pathway of each individual channel to be established. Channels were defined to terminate when
115 they were intersected by a larger, deeper routing pathway. We repeated this analysis for the Labyrinth channels which,
because of their size and anastomosing structure, are arguably the closest analogue for the channels submerged offshore
of Pine Island and Thwaites glaciers.

120 More than 2200 cross sections were analysed to determine the morphological characteristics of the
now-submarine Pine Island and Thwaites glacier channels, whilst more than 1600 were used to analyse the subaerially
exposed Labyrinth channels. Based on Noormets *et al.* (2009), we developed a semi-automated algorithm to quantify the
width, depth, cross-sectional area, and symmetry of each channel cross-section (Fig. 2). Channel width is defined as the
distance between the highest point of each of the channel sides. The greatest vertical distance between the base of the
channel and a line intersecting the two channel edges defines the channel depth, D . The horizontal distances from the
125 deepest point of the channel to each of the channel sides, $W1$ and $W2$, are calculated using an idealised triangular
representation of the channel. The normalised ratio of $W1$ to $W2$ is used to assess the symmetry of the channel, which can
range between 0 and 2. Symmetry values of 1 indicate a symmetrical cross-section, whilst values greater than 1 signify a
left-skewed channel and values less than 1 indicate a right-skewed channel cross section. Trapezoidal numerical



integration was used to approximate the internal area of the channel, bounded by the line intersecting the channel edges.

130 The ratio of channel depth to channel width was used to enable comparison between the vertical and horizontal proportions of each cross section.

In addition to the channel depth-width ratio, the cross-sectional shape of each sample was assessed using the General Power Law (GPL) program (Pattyn and Van Huelé, 1998). The GPL program applies a general form of the power-law equation to derive a best-fit approximation of a shape parameter, b , which summarises the geometric shape of the channel:

$$y - y_0 = a |x - x_0|^b \quad (1)$$

140 where a and b are constants, x_0 and y_0 are the coordinates of the origin of the cross section and x and y are the horizontal and vertical components of the channel cross section, respectively. A general least-squares method is used to derive the best-fit values of a and b . The value of the shape parameter, b , generally varies from 1 to 2 according to cross-sectional shape, with b -values of 1 indicating a ‘V-shaped’ cross section and values of 2 denoting a perfectly ‘U-shaped’ channel geometry (Pattyn and Van Huelé, 1998). Shape-parameter values exceeding 2 are associated with more box-shaped channel cross-sectional profiles, whereas geometries characterised by b -values less than 1 indicate channel flanks with a convex-upward form (Gales *et al.*, 2013).

2.3 Modelling past subglacial water flow

150 To assess the rates at which subglacial water could be produced, stored and routed beneath the former Pine Island and Thwaites glaciers, we performed hydrological modelling simulations for the full-glacial configuration of the Pine Island/Thwaites catchment, accounting for isostatic loading under the expanded WAIS, at 20 ka BP.

2.3.1 Palaeo ice-sheet reconstruction and data

155 The thickness and surface slope of the LGM configuration of the WAIS was derived from a series of palaeo ice-sheet reconstructions produced using the Parallel Ice Sheet Model (PISM) (Golledge *et al.*, 2012). PISM is a three-dimensional, thermomechanical ice-sheet model constrained by geological observations that has been widely used to simulate the dynamics of the Antarctic ice sheets (e.g. Golledge *et al.*, 2012, 2013, 2014; Fogwill *et al.*, 2014). PISM combines shallow-ice and shallow-shelf approximations for grounded ice to capture the dynamic behaviour of grounded ice and is able to simulate ice-stream flow and ice drawdown at a relatively high 5-km resolution (Golledge *et al.*, 2012; Fogwill *et al.*, 2014).

165 Simulation results from Golledge *et al.* (2012) provided the data required to calculate the routing and flux of subglacial water flowing under hydrostatic pressure beneath Pine Island and Thwaites glaciers at the LGM. A nested modelling approach was adopted in which catchment-wide water fluxes were first calculated at a 500-m resolution. These model results were then input at the edges of the higher-resolution bathymetric DEM covering the offshore channels. The bathymetric DEM was resampled to 90 m for the sake of computational efficiency. Ice-surface topography at the LGM was interpolated from the Golledge *et al.* (2012) reconstructions to the appropriate resolution (500 m or 90 m). Bed topography for the majority of the catchment was derived from the 500-m resolution BedMachine Antarctica dataset of the contemporary Antarctic Ice Sheet’s bed (Millan *et al.*, 2017; Morlighem *et al.*, 2018). These data were corrected for



isostasy by calculating the isostatic deflection at the LGM from the Golledge *et al.* (2012) results, and then adding the interpolated deflection values to the bed-topography data to produce a 500-m resolution, isostatically corrected DEM. Ice thickness was calculated by subtracting the interpolated ice-sheet surface from the isostatically-corrected bed topography. Subglacial topography and ice thickness were then used to calculate the subglacial hydraulic potential within the study region.

Basal meltwater production was calculated using the modelled basal frictional heating from the Golledge *et al.* (2012) reconstruction, added to the geothermal heat flux of the LGM Pine Island and Thwaites glaciers catchment. Geothermal heat flux values were derived from Martos *et al.* (2017) for the portion covered by the contemporary ice sheet and from Davies (2013) for the offshore portion of formerly ice-covered land. The geothermal heat flux of the catchment ranges between $\sim 70 \text{ mWm}^{-2}$ and $\sim 130 \text{ mWm}^{-2}$, whilst frictional heating values range from $\sim 0 \text{ mWm}^{-2}$ to $\sim 500 \text{ mWm}^{-2}$. For areas of the bed calculated to be at the pressure melting point in the Golledge *et al.* (2012) results, the sum of these heat sources was used to calculate the basal melt rate in each DEM cell, which can then be multiplied by the cell area to give a water volume per unit time. For cold-based ice where basal meltwater is absent, the production of basal meltwater was set to zero.

2.3.2 Flow routing

Meltwater routing beneath the $\sim 600,000 \text{ km}^2$ area drained by the LGM Pine Island and Thwaites glaciers catchment was modelled using a weighted upstream catchment area algorithm (Arnold, 2010; Willis *et al.* 2016). Subglacial hydraulic potential, Φ , dictates the flow and routing of water beneath ice masses (Shreve, 1972). The subglacial hydraulic potential of water flowing beneath an ice sheet is a function of bed topography and ice thickness:

$$\Phi = \rho_w g h + k \rho_i g Z \quad (2)$$

where ρ_w and ρ_i are the densities of water and ice (kg m^{-3}) respectively, g is the acceleration due to gravity (m s^{-2}), h is bed elevation (m), Z is ice thickness (m) and k is a dimensionless parameter (referred to as the uniform floatation factor) that can be varied from 0 to 1 to simulate variations in subglacial water pressure. Higher k values represent greater subglacial water pressure, with $k = 1$ denoting that water pressure is equal to the overburden pressure exerted by the overlying ice, and $k = 0$ representing water flowing at atmospheric pressure. Seismic (Blankenship *et al.*, 1986; Alley *et al.*, 1986) and borehole (Engelhardt *et al.*, 1990; Kamb, 2001; Tulaczyk *et al.*, 2001) investigations of the basal properties of Antarctic ice streams demonstrate that, where present, the pressure of subglacial meltwater is typically close to the ice-overburden pressure. Multibeam swath bathymetry, sub-bottom profiler, and coring studies have previously established that the now-submarine study area in Pine Island Bay was occupied by a major ice stream during the Last Glacial Maximum (e.g. Graham *et al.*, 2010). A k value of 0.995 was therefore chosen to parameterise subglacial water pressures within the numerical-model simulations to approximate the subglacial water pressures observed under contemporary Antarctic ice streams.

The upstream area model is described fully in Arnold (2010), and its adaptation for calculating the volume, throughput water discharge, and possible residence time of subglacial lakes is described in Willis *et al.* (2016). Briefly, the algorithm first identifies all cells in a hydraulic potential surface that have a lower potential than their neighbours. Such 'sink' cells allow local subglacial catchments (a group of contiguous cells which all drain toward the sink) to be



determined, and also form the nucleus for potential subglacial lakes. The algorithm ‘floods’ each sink cell to find the elevation of the lowest cell in the catchment surrounding the sink over which water would spill into a lower potential downstream cell (and hence, into an adjacent catchment). This spill point cell defines the maximum depth (relative to the sink), area and volume of each potential lake, and also allows the routing algorithm to pass the total catchment area (or cumulative subglacial melt) from catchment to catchment downstream until the model reaches the edge of the DEM. In this way, the algorithm builds up the topology of subglacial water flow, linking the individual catchments together into arborescent structures.

220

Rather than simply accumulating the DEM cell areas, the algorithm is weighted such that each cell contributes its modelled basal melt flux (see Section 2.3.1). This enables the steady-state subglacial water flux in each cell within the DEM, and the total discharge flowing into each potential subglacial lake, to be calculated. For each lake, the outflow discharge into the adjacent downstream catchment is set to be equal to the inflow discharge, as the algorithm assumes steady-state flow through each lake (which is assumed to be at maximum volume) in order to maintain topological continuity. By dividing the volume of each lake by the input water flux, the total time to refill the lake (again assuming steady flow) can be calculated. This effectively gives the minimum duration of any possible fill/drain cycle for each lake.

225

We compare our modelled continuous subglacial water fluxes to the theoretical discharge that could be accommodated by the channels if sufficient water was available based on channel cross-sectional area (Walder, 1986; Wingham *et al.*, 2006; Jordan *et al.*, 2010). The discharge, Q , of a semi-circular cross section, S , is equal to:

230

$$Q = 2 \left(\frac{\pi}{2} \right)^{\frac{1}{3}} S^{\frac{4}{3}} m^{-1} \left(\frac{\phi'}{p_w g} \right)^{\frac{1}{2}} \quad (3)$$

where ϕ' is the hydraulic potential gradient, p_w is the density of water (1000 kg m^{-3}), g is acceleration due to gravity (9.81 m s^{-2}), and m is the Manning coefficient ($0.08 \text{ m}^{-1/3} \text{ s}$). We derive S from the measured cross-sectional area of the channels in the multibeam bathymetry data and estimate along-channel estimates of ϕ' using Eq. (2). As the channels were unlikely to have been completely ice-free during periods of occupation by subglacial water, we calculate the hypothetical discharge under three scenarios in which the channel cross sections are: (1) ice-free, (2) 50 % occupied by ice, (3) 90 % occupied by ice.

240

3 Results

3.1 Morphology of channels in Pine Island Bay

245

Over 1000 channels were mapped within Pine Island Bay, covering an area of $\sim 19,000 \text{ km}^2$ (Fig. 3). The channels are arranged in a complex, anastomosing pattern that appears to follow lines of geological weakness in the inner-shelf bedrock. No channels are visible beyond the transition from the inner-shelf bedrock to the sedimentary strata on the outer continental shelf (e.g. Lowe and Anderson, 2003; Graham *et al.*, 2010; Nitsche *et al.*, 2013), $\sim 200 \text{ km}$ from the present ice margin. The channels are characterised by undulating long-axis profiles (thalwegs) containing multiple reverse gradients along their lengths. The majority of channels are less than 5000 m long, range in width from 80 m to 3400 m , and are incised into bedrock by between 3 m and 216 m . The channels are 560 m wide and 50 m deep on average, with a typical cross-sectional area of $20,000 \text{ m}^2$.

250



255 The bedrock channel system in Pine Island Bay is interspersed with a series of 19 flat-bottomed depressions with
steep sides relative to the gradient of their central floor. The depressions resemble a series of basins connected by the
channels. The basins range in planimetric area between 5 km² and 159 km² and descend several hundred metres beneath
the average depth of the surrounding topography. The basin floors contain subdued glacial landforms (Nitsche *et al.*,
2013) that appear to be partially buried by sedimentary infill.

260

3.2 Comparison with the Labyrinth

The channels offshore of present Pine Island and Thwaites glaciers are substantially larger than those comprising
the Labyrinth, which consists of a series of 80 channels that are generally less than 1000 m in length, 20 m to 600 m wide,
265 and 2 m to 150 m deep. The mean cross-sectional area of the Labyrinth channels is 3000 m². On average, the Labyrinth
channels are about half as deep and a third as wide as the Pine Island Bay channels at 23 m and 160 m, respectively
(Fig. 4). The two channel inventories are comparable in terms of their channel density, sinuosity, and characteristic
undulating longitudinal channel profiles; however, the channelised region of Pine Island Bay covers an area more than
400 times larger than the size of the Labyrinth (Figs. 3a–3d).

270

Both the Labyrinth and the Pine Island Bay channels tend to have asymmetric V-shaped (b -value = 1), rather
than U-shaped (b -value = 2), cross-sections. The bottom of the cross sections are commonly more V-shaped than the
upper sections of the channels. Channel cross-section depth-to-width ratios are also comparable in both regions, with
channels six to eight times wider than their depth (Fig. 4). For the Labyrinth channels, increasing cross-sectional area is
275 more strongly correlated with channel depth than channel width, suggesting that channel enlargement predominantly
results from disproportionate over-deepening of the larger channels with respect to their width. In contrast, increases in
Pine Island Bay channel area are due to both widening and deepening of channel cross sections.

280

3.3 Modelled subglacial hydrology

280

The numerical model results reveal an intricate system of water transfer and storage beneath the LGM
configuration of Pine Island and Thwaites glaciers (Fig. 5). The majority of the LGM catchment is estimated to be at the
pressure melting point. Predicted basal melt rates, which are dependent on ice-sheet thickness as well as geothermal and
strain heating, are greatest along the thick central and tributary trunks of the expanded Pine Island/Thwaites glaciers,
285 reaching values >50 mm yr⁻¹. The basin-wide average melt rate for the LGM catchment is ~20 mm yr⁻¹, producing a total
meltwater volume of 12.2 km³ per year. The hydraulic potential gradient of the LGM WAIS forces water northwards,
forming an arborescent drainage structure that converges into the main trunk of the formerly expanded Pine Island and
Thwaites glaciers. Numerous ponded water bodies are predicted to occur within the LGM catchment, several of which
fall within areas where subglacial water has been observed to transfer between subglacial lakes beneath the contemporary
290 WAIS (Smith *et al.*, 2017) (Fig. 5b).

The predicted subglacial water routing converges from across the catchment into the channelised region of Pine
Island Bay covered by high-resolution multibeam bathymetry (Fig. 5c). The majority of this water flow is routed
preferentially from beneath the present-day glacier margins and into the inner-shelf trough through the bedrock channels
295 (Fig. 5d). The majority of channels have a modelled steady state water discharge of less than 20 m³ s⁻¹. The highest



calculated continuous meltwater flux occurs in a channel situated in the centre of the trough with a discharge of $139 \text{ m}^3 \text{ s}^{-1}$ (Fig. 5c, location (i)).

Multiple lakes are predicted to occur in the bedrock depressions in Pine Island Bay under LGM conditions. Once the lakes are filled to their spill point, water is transferred through the bedrock channels into further lakes downstream. We examine the modelled fluxes, volumes, and recharge rates of the lakes using four examples displayed in Fig. 5c. Lake (i) occurs at the confluence of the main streams that drain the Pine Island and Thwaites glaciers catchments; lake (ii) is the furthest downstream lake in the Thwaites catchment, and lake (iii) is the furthest downstream lake in the Pine Island catchment. The fourth example lake occurs within the relict subglacial lake basin described by Kuhn *et al.* (2017). The four example lakes have volumes between 0.33 km^3 and 19.9 km^3 when filled to their spill points. The majority of the water routed into Pine Island Bay is directed from beneath Thwaites Glacier, flowing into lake (ii) at a steady-state rate of $101 \text{ m}^3 \text{ s}^{-1}$. When combined with the steady-state flux of water contributed by the Pine Island Glacier catchment ($32.2 \text{ m}^3 \text{ s}^{-1}$), the two catchments yield a steady-state discharge of $139 \text{ m}^3 \text{ s}^{-1}$ through lake (i). Under these continuous flow rates, the three lakes would fill to their spill points on annual to decadal timescales (Table 2). The basin described by Kuhn *et al.* (2017) is smaller than the lakes draining the main glacier catchments and is modelled to accumulate water at a steady state rate of $0.23 \text{ m}^3 \text{ s}^{-1}$, filling to its spill point every 45 years. If these example lakes were to drain over a ~ 16 month period, typical of subglacial water transfer beneath the contemporary Antarctic Ice Sheet (Wingham *et al.*, 2006), water would be released from the lakes at an average rate of $\sim 10\text{--}80 \text{ m}^3 \text{ s}^{-1}$ for the three smaller lakes (i, ii, iv) and $\sim 470 \text{ m}^3 \text{ s}^{-1}$ for lake (iii) at the edge of the individual Pine Island glacier catchment (Table 2).

We quantify the largest possible discharge that could occur through the channels by considering a scenario in which a large modelled lake, situated upstream in the Pine Island/Thwaites catchment, drains within 16 months and triggers a cascade of catastrophic lake drainages downstream. This scenario represents the most extreme discharge that could have been generated beneath the LGM configuration of Pine Island and Thwaites glaciers. Under this scenario, the mean flood discharge through the inner shelf channels would be $\sim 5.5\text{--}6.6 \times 10^4 \text{ m}^3 \text{ s}^{-1}$. However, these are mean discharges. In a modelling study of water transfer between subglacial lakes in the Adventure subglacial trench, using data from Wingham *et al.* (2006), Peters *et al.* (2009) found that subglacial discharge between the lakes was highly sensitive to the model parameters used, especially the assumed channel roughness, and short-lived peak fluxes of around ten times the mean discharge were quite conceivable. Given this uncertainty, it may have been possible to produce short-lived outbursts up to $\sim 5 \times 10^5 \text{ m}^3 \text{ s}^{-1}$ through the Pine Island Bay channels. This estimate is of the order of 10 % to 50 % of the maximum carrying capacity of the channels (Eq. (3)). Under the hydraulic potential gradient of the LGM configuration of the WAIS, channels filled with water to the bankfull stage would be capable of accommodating flows with an average discharge of $\sim 8.8 \times 10^6 \text{ m}^3 \text{ s}^{-1}$. This carrying capacity would be reduced to $3.5 \times 10^6 \text{ m}^3 \text{ s}^{-1}$ if the channels were 50 % ice filled, and to $2.8 \times 10^5 \text{ m}^3 \text{ s}^{-1}$ if they were 90 % ice filled.

5 Discussion

5.1 Channel formation

The morphology, discharge carrying capacity, and form distributions of the Pine Island Bay and Labyrinth channels are strikingly similar despite the former being significantly larger. The undulating long-axis profiles and reverse gradients associated with both channel inventories, combined with their size, shape, and their incision into bedrock



suggests that they were formed by high-velocity subglacial meltwater flowing under hydrostatic pressure (Shreve, 1972; Sugden *et al.*, 1991; Lowe and Anderson, 2003; Lewis *et al.*, 2006; Smith *et al.*, 2009b; van der Vegt *et al.*, 2012; Nitsche *et al.*, 2013). Morphometric evidence thus indicates a similar formative process for both sets of channels; that is, incision
340 by pressurised subglacial water, albeit executed over a vastly larger scale beneath Pine Island and Thwaites glaciers than at the Labyrinth (Fig. 3).

The dimensions and the extensive area over which the submarine channels are observed indicates that the
345 hydrological system beneath the formerly expanded Pine Island and Thwaites glaciers at times transported substantial volumes of pressurised water along consistent routing pathways. The transportation of coarse bedload permits water to rapidly incise bedrock (Cook *et al.*, 2013a). In order to mobilise such suitable sediment loads, large fluxes of water would have been required to excavate channels of the size observed in Pine Island Bay (Alley *et al.*, 1997). Although it is likely that infilling with ice prevented all of the channels from being active contemporaneously (Nitsche *et al.*, 2013), even if
350 half of the channel cross sections were filled with grounded ice, at $3.5 \times 10^6 \text{ m}^3 \text{ s}^{-1}$, their carrying capacity would still have been larger than the maximum bankfull discharge estimated for the Labyrinth ($1.6\text{--}2.2 \times 10^6 \text{ m}^3 \text{ s}^{-1}$) (Lewis *et al.*, 2006). Constraining the age of submarine channels is difficult; however, the presence of deformation till in some of the channels indicates that they have been overridden by wet-based ice since their incision so may be the outcome of several advances and retreats of grounded ice through Pine Island Bay (Smith *et al.*, 2009b; Nitsche *et al.*, 2013).

355 Unlike the channels in Pine Island Bay, the age and formation of the Labyrinth is better constrained, and has been attributed to one or more subglacial floods sourced from a subglacial lake trapped as the Antarctic Ice Sheet overrode the Transantarctic Mountains during the Miocene (Lewis *et al.*, 2006). The last period of Labyrinth channel incision occurred between 14.4 Ma BP and 12.4 Ma BP (Marchant *et al.*, 1993, 1996; Denton and Sugden, 2005; Lewis *et al.*,
360 2006). Around this time, the region experienced strong climatic cooling of at least 8°C (Lewis *et al.*, 2007, 2008). This period of cooling changed the basal thermal regime of the ice in the vicinity of the Labyrinth to minimally erosive cold-based ice, potentially protecting the channels from any substantial further erosion (Atkins and Dickinson, 2007). The absence of post-incisional reworking of the top of the channels by wet-based ice may explain the tendency for increased Labyrinth channel cross-sectional area to be more strongly correlated with channel depth than channel width.
365 In contrast, increasing cross-sectional area of the channels in Pine Island Bay is correlated with both channel width and depth, suggesting that glacial erosion of the sides of the channels has been a significant additional process influencing the morphology of the channels. This supports the notion that the channels have been formed and reoccupied over multiple glacial cycles, allowing subglacial erosion to enlarge the top of the channels (Fig. 6). Interestingly, this implies that the Labyrinth channels may represent ‘purer’ meltwater signatures than the larger features observed in Pine Island Bay.

370

5.2 Channel water sources

The polar desert climate characterising the contemporary Antarctic Ice Sheet largely prevents the production of surface meltwater (Rose *et al.*, 2014). Even where seasonal surface melting occurs, such as along portions of the Antarctic
375 Peninsula and on low-latitude East Antarctic ice shelves (Barrand *et al.*, 2013; Trusel *et al.*, 2013; Bell *et al.*, 2018), water may be transported efficiently across the ice surface through the action of surficial meltwater rivers (Bell *et al.*, 2017; Kingslake *et al.*, 2017). This results in the meltwater failing to enter the englacial or subglacial hydrological system. With average summer temperatures around -10°C at the present-day coast around Pine Island Bay (King and Turner, 2007), the contribution of surface meltwater to the subglacial hydrological system can be considered negligible if the past climate



380 were similar to present, or more likely colder, under late Pleistocene full-glacial conditions (Trusel *et al.*, 2013). Therefore, even assuming a climate similar to present, the subglacial meltwater responsible for bedrock-channel formation could only have been generated by geothermal and strain heating at the ice-sheet bed.

385 The geothermal heat flux beneath West Antarctica is larger than for the remainder of the continent due to its location on the West Antarctic Rift System — an extensional volcanic rift system that stretches across Marie Byrd Land from Pine Island Glacier and into the Ross Sea (Blankenship *et al.*, 1993; LaMasurier, 2013; Loose *et al.*, 2018). Despite this elevated geothermal heat flux, the quantity of subglacial meltwater produced by geothermal heating is estimated to be only 4–10 mm yr⁻¹ (Dowdeswell *et al.*, 2016) — two orders of magnitude less than the maximum rates of surface melt observed on the Antarctic Peninsula today (>400 mm yr⁻¹ w.e.) (Trusel *et al.*, 2013). Although basal melt rates may be 390 elevated by strain heating at the lateral shear-margins of ice streams (Bell, 2008; Graham *et al.*, 2009), the combination of these processes would only yield subglacial melt rates of up to 90–180 mm yr⁻¹ (Dowdeswell *et al.*, 2016).

The basin-wide average basal meltwater production rate beneath Pine Island and Thwaites glaciers is ~28 mm yr⁻¹ at present, generating 5.2 km³ of meltwater per year (Joughin *et al.*, 2009). Our model calculates that under 395 the LGM configuration of these glaciers, meltwater would have been produced at ~20 mm yr⁻¹ on average, although elevated melt rates >50 mm yr⁻¹ would have occurred beneath the thick central ice-stream tongue. Combined, these melt rates would have generated a total volume of 12.2 km³ per year across the entire LGM catchment. These rates are too low to transport sediment efficiently and would therefore preclude significant erosion of bedrock (Alley *et al.*, 1997). Furthermore, there is a discrepancy between the potential carrying capacity of the channels and the predicted discharges 400 through the channels if the subglacial water-transfer system is assumed to be in steady state. This discrepancy occurs because the channels, even if 90 % full of ice, would be capable of accommodating discharges over three orders of magnitude larger ($2.8 \times 10^5 \text{ m}^3 \text{ s}^{-1}$) than the largest steady state water fluxes predicted to occur by the numerical model (139 m³ s⁻¹). The continuous production of basal meltwater beneath former Pine Island and Thwaites glaciers is therefore insufficient to incise channels of the size present in Pine Island Bay (Lowe and Anderson, 2003; Nitsche *et al.*, 2013). 405 Consequently, another mechanism, capable of mobilising coarse bedload, is required to explain their formation.

Episodic, but high-magnitude, subglacial volcanic activity occurring over multi-millennial timescales may have supplied large volumes of meltwater to the subglacial hydrological system of Pine Island and Thwaites glaciers in the past (Wilch *et al.*, 1999; Nitsche *et al.*, 2013). West Antarctica contains 138 volcanoes, including three extensively eroded 410 Miocene volcanoes and other younger parasitic cones in the Hudson Mountains, 150 km east of Pine Island Bay (Nitsche *et al.*, 2013; Van Wyk de Vries *et al.*, 2017; Loose *et al.*, 2018). The most recent volcanic eruption in this region occurred ~2200 years ago (Corr and Vaughan, 2008). Analogies from subglacial volcanic eruptions in Iceland demonstrate that these events commonly cause meltwater to accumulate in unstable subglacial lakes incised upwards into the ice (Björnsson, 1992, 2002). When hydrostatic pressure exceeds the strength of the ice damming the lake, jökulhlaup outburst 415 floods may occur with discharges of up to $5 \times 10^4 \text{ m}^3 \text{ s}^{-1}$ (Björnsson, 2002). Jökulhlaups transport huge amounts of sediment, in the order of 10,000,000 tonnes, per event (Nye, 1976; Roberts, 2005) allowing them to impose a significant geomorphic imprint upon the landscape, including the incision of large subglacial channels (Björnsson, 2002; Russell *et al.*, 2007). However, although it is possible that volcanically induced subglacial floods supplied large volumes of water to the beds of Pine Island and Thwaites glaciers in the past, this mechanism does not explain the occurrence of channelised 420 landforms observed in different, less volcanically active, regions of Antarctica such as the East Antarctic Soya Coast (Sawagaki and Hirakawa, 1997) and the western Antarctic Peninsula (e.g. Ó Cofaigh *et al.*, 2002, 2005; Domack *et al.*,



2006; Anderson and Oakes-Fretwell, 2008). Hence, although episodic volcanism may have contributed water to the formation of the channel system present in Pine Island Bay, it is unlikely to represent the sole or dominant mechanism through which the channels formed.

425

Meltwater features, similar to the channels in Pine Island Bay, have been mapped and modelled beneath other former ice sheets such as the Fennoscandian and Barents Sea ice sheets (Greenwood *et al.*, 2016, 2017; Bjarnadóttir *et al.*, 2017; Shackleton *et al.*, 2018), the Laurentide Ice Sheet (Bretz, 1923, 1969; Livingstone *et al.*, 2013a, 2016; Livingstone and Clark, 2016), and the British-Irish Ice Sheet (Sissons, 1958; Clark *et al.*, 2004; Greenwood *et al.*, 2007).

430

The deglacial configuration of these former ice sheets was likely conducive to producing large volumes of surface meltwater that may have propagated to the bed (Carlson *et al.*, 2008; Jansen *et al.*, 2014), similar to that observed on the margins of the contemporary Greenland Ice Sheet (Zwally *et al.*, 2002; Das *et al.*, 2008; Bartholomew *et al.*, 2012). Subglacial streams fed by surface melt have high discharges and an exceptional sediment transport capacity due to the short time period in which supraglacial drainage occurs (Alley *et al.*, 1997). When this water is delivered to portions of

435

the bed where unconsolidated sediments have been stripped away, these high water-fluxes will have very large unsatisfied transport capacities and will be able to rapidly erode bedrock if paired with a suitable bedload (Alley *et al.*, 1997; Cook *et al.*, 2013a). Exceptionally high erosion rates have been associated with supraglacial water input to the Greenland subglacial hydrological system (Cowton *et al.*, 2012), and the input of supraglacial meltwater into the subglacial hydrological system of the deglaciating Fennoscandian Ice Sheet has been proposed to have cut large undulating gorges

440

into bedrock in northern Sweden (Jansen *et al.*, 2014).

Although the injection of surface meltwater to the bed of the Antarctic Ice Sheet through hydrofracture is potentially forecast under future climate warming scenarios (Bell *et al.*, 2018), the extent to which surface melting of the Antarctic Ice Sheet may have occurred in the past is poorly constrained. However, evidence from environmental proxies (Escutia *et al.*, 2009; Cook *et al.*, 2013b), sea-level reconstructions (Miller *et al.*, 2012) and numerical-modelling simulations (DeConto and Pollard, 2003) indicates that significant circum-Antarctic warming occurred during the Miocene and the Pliocene (5.3–2.6 Ma BP) epochs. This climate warming may have raised surface temperatures sufficiently to facilitate surface melt across significant portions of the Antarctic interior (Rose *et al.*, 2014). However, numerical-model simulations suggest that despite peak Miocene air temperatures being sufficiently warm to facilitate surface melting, it is unlikely that the WAIS was developed enough at this time to allow large-scale grounded ice to extend onto the inner continental shelf of the Amundsen Sea, precluding the possibility of subglacial channel formation in Pine Island Bay (DeConto and Pollard, 2003).

445

450

The establishment of a more expansive, yet dynamic (Cook *et al.*, 2013b), WAIS during the Pliocene (Pollard and DeConto, 2009; DeConto and Pollard, 2016), combined with temperatures 2°C to 3°C warmer than present (Dowsett, 2007), make this epoch a potential candidate for when substantial quantities of surficial meltwater could propagate to the bed of the WAIS and form the meltwater channels. Ice-sheet modelling by Raymo *et al.* (2006) predicts that the extent of Pliocene summer melting on the East Antarctic Ice Sheet margin would have been comparable to the considerable quantities of supraglacial meltwater produced during the summer ablation season of the contemporary Greenland Ice Sheet (e.g. Abdalati and Steffen, 2001; Zwally *et al.*, 2002; Hanna *et al.*, 2008). If a comparable level of surface melt also occurred on the surface of the WAIS at this time, substantial quantities of supraglacial meltwater could have propagated to the expanded ice sheet's bed, facilitating channel incision (Rose *et al.*, 2014). Although bedrock channels exist on the Greenland continental shelf (Ó Cofaigh *et al.*, 2004; Dowdeswell *et al.*, 2010) and beneath the contemporary Greenland

460



465 Ice Sheet (Bamber *et al.*, 2013), they are not nearly as common as those offshore of the WAIS and the formation of many
has been attributed to turbidity currents or fluvial activity predating the inception of the Greenland Ice Sheet (e.g.
Batchelor *et al.*, 2018). Accordingly, if supraglacial water injection is responsible for the incision of the Antarctic channels,
it raises the question of why these features are not more common on the margin of the Greenland Ice Sheet where this
process is known to occur, or why channels have not been observed forming beneath the contemporary ice sheet today.

470 An alternative source of water with which the channels could have formed is subglacial lakes produced by the
accumulation of subglacial meltwater in hydraulic potential lows. The seafloor of Pine Island Bay and the bed of the LGM
catchment contains multiple bedrock basins where low hydraulic potential provides favourable locations for water to pond
beneath the WAIS at the LGM (Fig. 5). The dimensions of the basins beyond the current Pine Island/Thwaites glacier
margins are of the same order of magnitude as many contemporary subglacial lakes occupying bedrock basins. For
475 example, Lake Ellsworth has an area of 29 km² (Siegert *et al.*, 2004) whereas the basins beyond PIG and TG have
planimetric areas between 5 km² and 160 km². The modelled water bodies have volumes, filling/drainage times, and
steady state inflow and outflow fluxes that are comparable to contemporary subglacial lake drainage events observed
using satellite altimetry (Wingham *et al.*, 2006; Fricker *et al.*, 2007; Flament *et al.*, 2014; Smith *et al.*, 2017). The bedrock
basins in Pine Island Bay are infilled with several to tens of metres of sediment (Nitsche *et al.*, 2013). Sediments recovered
480 from one of these basins suggest deposition in a low energy freshwater subglacial lake environment during the last glacial
period (Kuhn *et al.*, 2017), an interpretation that is consistent with the low magnitude water flux modelled for the basin
sampled (0.23 m³ s⁻¹). Consequently, similar to other areas offshore of the Antarctic Peninsula (Domack *et al.*, 2006), it
is possible that the bedrock basins in Pine Island Bay may represent the locations of relict subglacial lakes in past glacial
periods (Domack *et al.*, 2006; Livingstone *et al.*, 2013b; Kuhn *et al.*, 2017).

485 Although multiple subglacial lake drainage events have been observed beneath the contemporary Antarctic Ice
Sheet (e.g. Gray *et al.*, 2005; Wingham *et al.*, 2006; Fricker *et al.*, 2007; Smith *et al.*, 2009a, 2017), the peak discharge
and volume of water displaced during contemporary lake drainage is four to five orders of magnitude smaller than the
amount that we predict the channels in Pine Island Bay could accommodate, even when mostly filled with ice.
490 Furthermore, models of active subglacial lake drainage most closely replicate observed subglacial lake behaviour when
water mechanically erodes shallow canals into underlying deformable sediment rather than producing an R-channel
(Röthlisberger, 1972) type drainage mechanism (Fowler, 2009; Carter *et al.*, 2009, 2017). These results are consistent
with measured pore water pressures beneath Whillans Ice Stream (Blankenship *et al.*, 1987; Engelhardt *et al.*, 1990;
Walder and Fowler, 1994; Alley *et al.*, 1997), and radar specular analysis of present-day Thwaites Glacier although, in
495 the case of the latter, it is possible that a focused channelised system exists further downstream (Schroeder *et al.*, 2013).
These observations may imply that many active subglacial lakes require soft bedded sediments to form and drain (Carter
et al., 2017), explaining the tendency for these features to lack the characteristic basal reflection properties used to identify
subglacial lakes with radio-echo sounding (Siegert *et al.*, 2015; Carter *et al.*, 2017; Humbert *et al.*, 2018). However, it
may be possible to produce, and temporarily sustain, R-channels with cross-sectional areas of ~20 m² when water is
500 transferred between a system of bedrock overdeepenings by pressure waves that propagate along the length of an ice
stream over several years (Fricker *et al.*, 2014; Dow *et al.*, 2018), or along ice stream shear margins where basal meltwater
production rates are high (Perol *et al.*, 2015; Elsworth and Suckale, 2016; Meyer *et al.*, 2016; Bougamont *et al.*, 2018).

505 The extent to which the active subglacial lake drainage events observed in the satellite era are representative of
the behaviour of the Antarctic subglacial hydrological system over a full-glacial/interglacial cycle, especially during



ice-sheet advance and retreat, is unknown. However, it is clear that, due to the volume of water and the inferred drainage mechanism involved, the contemporary drainage of active subglacial lakes could not incise channels of the size observed in Pine Island Bay into bedrock, even if drainage was periodically repeated over multi-millennial timescales. Hence, if a lake drainage mechanism is invoked to explain the formation of the Pine Island Bay channels, it would need to be different
510 to the water transfer mechanism observed between active subglacial lakes at present.

Several landscapes in Antarctica have been attributed to large floods sourced from subglacial lakes. Jordan *et al.* (2010) proposed that outbursts sourced from a palaeo-subglacial lake with a volume of 850 km³ were responsible for the formation of a series of kilometre-wide bedrock canyons in the Wilkes Subglacial Basin. This lake is proposed to have
515 accumulated and drained during the expansion of the East Antarctic Ice Sheet in the Miocene epoch, at a similar time to when the Labyrinth and the other channel systems in Victoria Land are suggested to have formed (Denton *et al.*, 1984, 1993; Sugden *et al.*, 1999; Sugden and Denton, 2004; Denton and Sugden, 2005). Morphological evidence for past outburst flood occurrence also exists elsewhere in Scandinavia (Mannerfelt, 1945; Holtedahl, 1967), in North America (Bretz, 1923; Ives, 1958; Wright, 1973) and in Scotland (Sissons, 1958). The largest of these floods was the release of
520 ~2500 km³ of water during the Missoula floods in eastern Washington State, USA, which have been estimated to have attained peak discharges of $\sim 1.7 \times 10^7 \text{ m}^3 \text{ s}^{-1}$ (Waitt, 1985; O'Connor and Baker, 1992). This volume is similar to the amount of water that could be utilised beneath former Pine Island and Thwaites glaciers if a cascade of upstream lake drainage was to occur (Table 2).

Two models of how Antarctic lakes could form and then drain catastrophically have been hypothesised. Alley
525 *et al.* (2006) proposed a model in which seawater becomes trapped in bedrock basins by the advance and thickening of an ice shelf over the sill of bedrock overdeepenings. Water pressure in the basins would build until the hydraulic potential exceeds that of the next basin downstream, culminating in short-lived, high-magnitude water drainage events, or floods. An alternative hypothesis was put forward by Jordan *et al.* (2010) in which subglacial water ponds in hydraulic-potential
530 lows produced by the reduced ice-surface slope associated with an advancing ice sheet, with flooding occurring during ice-sheet retreat (Jordan *et al.*, 2010). Both of these lake-drainage models occur during either large-scale ice sheet advance or retreat, so are outside of the subglacial hydrodynamics captured by modern observations. Numerical calculations show that these types of event are capable of producing peak discharges of $\sim 10^5 \text{ m}^3 \text{ s}^{-1}$ (Evatt *et al.*, 2006). Our numerical model
535 results demonstrate that the cascading release of water trapped in a large upstream basin could initiate a flood with a peak discharge of $\sim 5 \times 10^5 \text{ m}^3 \text{ s}^{-1}$. This discharge is approximately equal to the potential carrying capacity of the channels if they were partially ice filled at the time of the flood. If repeated over multiple glacial cycles, these water fluxes would have been sufficient to excavate large channels in bedrock when paired with a suitable sediment load for channel erosion. If the more catastrophic forms of lake drainage are invoked to have occurred during either ice sheet advance or retreat, the combination of coarse bedload derived from direct glacial erosion and short-lived, high-magnitude drainage from a
540 population of subglacial lakes occupying large bedrock basins over multiple glacial-deglacial cycles may have been sufficiently erosive to excavate huge channels in the bedrock of Pine Island Bay.

6 Conclusion

545 The huge palaeo-channel-and-basin systems beyond modern Pine Island and Thwaites glaciers are evidence for an organised and dynamic subglacial hydrological system beneath former major outlets of the WAIS. Channels of greater dimensions than those in the Labyrinth can only have been incised by high-magnitude discharges of water flowing under



subglacial hydraulic pressure. Our numerical model produces similar steady-state discharges and filling and drainage
timescales to those that are observed for subglacial lakes beneath the contemporary Antarctic Ice Sheet. However, the
550 fluxes of water flowing in continuous steady state beneath the LGM ice sheet are too low to have formed channels of the
scale observed in Pine Island Bay. Rather, a high-magnitude, low-frequency mechanism is required to explain the
formation of the channels. Many mechanisms could have been responsible for channel formation, including propagation
of surface melt to the bed and subglacial volcanic eruptions. However, we have argued that on the basis of their
geomorphological similarity to features known to have been formed by catastrophic outburst flooding and their ability to
555 accommodate discharges of at least $2.8 \times 10^5 \text{ m}^3 \text{ s}^{-1}$, even when mostly filled with ice, the most likely candidate for the
formation of the Pine Island Bay channel system was episodic releases of meltwater trapped in upstream subglacial lakes
triggered by ice-sheet advance or retreat. This mechanism is probably outside the range of processes captured by modern
observations of subglacial hydrology, but is likely to have had an impact on the flow regime of these large ice streams
that continue to dominate ice-sheet discharge today. Further observations of the duration and frequency of contemporary
560 subglacial drainage events and the incorporation of more detailed bed topographies into numerical models will help
elucidate the role that organised, episodic outburst flooding plays in the dynamics of the Antarctic Ice Sheet.

565

570

575

580

585



590 **References**

- Abdalati, W. and Steffen, K.: Greenland ice sheet melt extent: 1979–1999. *Journal of Geophysical Research: Atmospheres*. 106(D24), 33983-33988. <https://doi.org/10.1029/2001JD900181>, 2001.
- 595 Alley, R.B., Blankenship, D.D., Bentley, C.R. and Rooney, S.: Deformation of till beneath ice stream B, West Antarctica. *Nature*. 322(6074), 57-59. <https://doi.org/10.1038/322057a0>, 1986.
- Alley, R.B., Cuffey, K.M., Evenson, E.B., Strasser, J.C., Lawson, D.E. and Larson, G.J.: How glaciers entrain and transport basal sediment: physical constraints. *Quaternary Science Reviews*, 16(9), 1017-1038.
600 [https://doi.org/10.1016/S0277-3791\(97\)00034-6](https://doi.org/10.1016/S0277-3791(97)00034-6), 1997.
- Alley, R.B., Dupont, T.K., Parizek, B.R., Anandakrishnan, S., Lawson, D.E., Larson, G.J. and Evenson, E.B.: Outburst flooding and the initiation of ice-stream surges in response to climatic cooling: A hypothesis. *Geomorphology*. 75(1), 76-89. <https://doi.org/10.1016/j.geomorph.2004.01.011>, 2006.
605
- Anderson, J.B. and Oakes-Fretwell, L.: Geomorphology of the onset area of a paleo-ice stream, Marguerite Bay, Antarctic Peninsula. *Earth Surface Processes and Landforms*. 33(4), 503-512. <https://doi.org/10.1002/esp.1662>, 2008.
- 610 Arnold, N.: A new approach for dealing with depressions in digital elevation models when calculating flow accumulation values. *Progress in Physical Geography*. 34(6), 781-809. <https://doi.org/10.1177/0309133310384542>, 2010.
- Atkins, C.B. and Dickinson, W.W.: Landscape modification by meltwater channels at margins of cold-based glaciers, Dry Valleys, Antarctica. *Boreas*, 36(1), 47-55. <https://doi.org/10.1080/03009480600827306>, 2007.
- 615 Bamber, J.L., Siegert, M.J., Griggs, J.A., Marshall, S.J. and Spada, G.: Paleofluvial Mega-Canyon Beneath the Central Greenland Ice Sheet. *Science*, 341, 997-999. <https://doi.org/10.1126/science.1239794>, 2013.
- 620 Barrand, N.E., Vaughan, D.G., Steiner, N., Tedesco, M., Kuipers Munneke, P., van den Broeke, M.R. and Hosking, J.S.: Trends in Antarctica Peninsula surface melting conditions from observations and regional climate modelling. *Journal of Geophysical Research: Earth Surface*, 118(1). <https://doi.org/10.1029/2012JF002559>, 2013.
- 625 Bartholomew, I., Nienow, P., Sole, A., Mair, D., Cowton, T. and King, M.A.: Short-term variability in Greenland Ice Sheet motion forced by time-varying meltwater drainage: Implications for the relationship between subglacial drainage system behavior and ice velocity. *Journal of Geophysical Research: Earth Surface*, 117(F3). <https://doi.org/10.1029/2011JF002220>, 2012.



- 630 Batchelor, C.L., Dowdeswell, J.A. and Rignot, E.: Submarine landforms reveal varying rates and styles of deglaciation in North-West Greenland fjords. *Marine Geology*, 402, 60-80. <https://doi.org/10.1016/j.margeo.2017.08.003>, 2018.
- Bell, R.E., Studinger, M., Shuman, C.A., Fahnestock, M.A. and Joughin, I.: Large subglacial lakes in East Antarctica at the onset of fast-flowing ice streams. *Nature*, 445(7130), 904-907. <https://doi.org/10.1038/nature05554>, 2007.
- 635 Bell, R.E.: The role of subglacial water in ice-sheet mass balance. *Nature Geoscience*. 1(5), 297-304. <https://doi.org/10.1038/ngeo186>, 2008.
- 640 Bell, R.E., Chu, W., Kingslake, J., Das, I., Tedesco, M., Tinto, K.J., Zappa, C.J., Frezzotti, M., Boghosian, A. and Lee, W.S.: Antarctic ice shelf potentially stabilized by export of meltwater in surface river. *Nature*, 544(7650), 344-348. <https://doi.org/10.1038/nature22048>, 2017.
- Bell, R.E., Banwell, A.F., Trusel, L.D. and Kingslake, J.: Antarctic surface hydrology and impacts on ice-sheet mass balance, *Nature Climate Change*. <https://doi.org/10.1038/s41558-018-0326-3>, 2018.
- 645 Bjarnadóttir, L.R., Winsborrow, M.C.M. and Andreassen, K.: Large subglacial meltwater features in the central Barents Sea. *Geology*, 45(2). 159-162. <https://doi.org/10.1130/G38195.1>, 2017.
- 650 Björnsson, H.: Jökulhlaups in Iceland: prediction, characteristics and simulation. *Annals of Glaciology*, 16, 95-106. <https://doi.org/10.3189/1992AoG16-1-95-106>, 1992.
- Björnsson, H.: Subglacial lakes and jökulhlaups in Iceland. *Global and Planetary Change*, 35(3-4), 255-271. [https://doi.org/10.1016/S0921-8181\(02\)00130-3](https://doi.org/10.1016/S0921-8181(02)00130-3), 2002.
- 655 Blankenship, D.D., Bentley, C.R., Rooney, S.T. and Alley, R.B.: Seismic measurements reveal a saturated porous layer beneath an active Antarctic ice stream. *Nature*. 322(6074), 54-57. <https://doi.org/10.1038/322054a0>, 1986.
- 660 Blankenship, D.D., Bentley, C.R., Rooney, S.T. and Alley, R.B.: Till beneath Ice Stream B: 1. Properties derived from seismic travel times. *Journal of Geophysical Research: Solid Earth*, 92(B9), 8903-8911. <https://doi.org/10.1029/JB092iB09p08903>, 1987.
- 665 Blankenship, D. D., Bell, R. E., Hodge, S. M., Brozena, J. M., Behrendt, J. C., and Finn, C. A.: Active volcanism beneath the West Antarctic ice sheet and implications for ice-sheet stability. *Nature*. 361, 526-529. <https://doi.org/10.1038/361526a0>, 1993.
- Bougamont, M., Christoffersen, P., Nias, I., Vaughan, D.G., Smith, A.M. and Brisbourne, A.: Contrasting hydrological controls on bed properties during the acceleration of Pine Island Glacier, West Antarctica. *Journal of Geophysical Research*, 124(1). <https://doi.org/10.1029/2018JF004707>, 2018.
- 670



- Bretz, J.H.: The channeled scablands of the Columbia Plateau. *The Journal of Geology*. 31(8), 617-649.
<https://doi.org/10.1086/623053>, 1923.
- 675 Bretz, J.H.: The Lake Missoula floods and the channeled scabland. *The Journal of Geology*. 77(5), 505-543.
<https://doi.org/10.1086/627452>, 1969.
- Carlson, A.E., LeGrande, A.N., Oppo, D.W., Came, R.E., Schmidt, G.A., Anslow, F.S., Licciardi, J.M. and Obbink, E.A.:
Rapid early Holocene deglaciation of the Laurentide ice sheet. *Nature Geoscience*, 1, 620-624,
<https://doi.org/10.1038/ngeo285>, 2008.
- 680 Carter, S.P., Blankenship, D.D., Young, D.A., Peters, M.E., Holt, J.W. and Siegert, M.J.: Dynamic distributed drainage
implied by the flow evolution of the 1996–1998 Adventure Trench subglacial lake discharge. *Earth and Planetary
Science Letters*, 283(1-4), 24-37. <https://doi.org/10.1016/j.epsl.2009.03.019>, 2009.
- 685 Carter, S.P., Fricker, H.A. and Siegfried, M.R.: Antarctic subglacial lakes drain through sediment-floored canals: theory
and model testing on real and idealized domains. *The Cryosphere*, 11(1), 381-405. <https://doi.org/10.5194/tc-11-381-2017>, 2017.
- Clark, C. D., Evans, D. J., Khatwa, A., Bradwell, T., Jordan, C. J., Marsh, S.H., Mitchell, W.A. and Bateman, M.D.: Map
and GIS database of glacial landforms and features related to the last British Ice Sheet. *Boreas*, 33, 359–375,
<https://doi.org/10.1111/bor.12273>, 2004.
- 690 Clark, C. D., Evans, D. J., Khatwa, A., Bradwell, T., Jordan, C. J., Marsh, S.H., Mitchell, W.A. and Bateman, M.D.: Map
and GIS database of glacial landforms and features related to the last British Ice Sheet. *Boreas*, 33, 359–375,
<https://doi.org/10.1111/bor.12273>, 2004.
- Cook, K.L., Turowski, J.M. and Hovius, N.: A demonstration of the importance of bedload transport for fluvial bedrock
erosion and knickpoint propagation. *Earth Surface Processes and Landforms*, 38(7), 683-695.
<https://doi.org/10.1002/esp.3313>, 2013a.
- 695 Cook, K.L., Turowski, J.M. and Hovius, N.: A demonstration of the importance of bedload transport for fluvial bedrock
erosion and knickpoint propagation. *Earth Surface Processes and Landforms*, 38(7), 683-695.
<https://doi.org/10.1002/esp.3313>, 2013a.
- Cook, C.P., Van De Flierdt, T., Williams, T., Hemming, S.R., Iwai, M., Kobayashi, M., Jimenez-Espejo, F.J., Escutia, C.,
González, J.J., Khim, B.K. and McKay, R.M.; Dynamic behaviour of the East Antarctic ice sheet during Pliocene
warmth. *Nature Geoscience*. 6(9), 765-769. <https://doi.org/10.1038/ngeo1889>, 2013b.
- 700 Cook, C.P., Van De Flierdt, T., Williams, T., Hemming, S.R., Iwai, M., Kobayashi, M., Jimenez-Espejo, F.J., Escutia, C.,
González, J.J., Khim, B.K. and McKay, R.M.; Dynamic behaviour of the East Antarctic ice sheet during Pliocene
warmth. *Nature Geoscience*. 6(9), 765-769. <https://doi.org/10.1038/ngeo1889>, 2013b.
- Corr, H.F. and Vaughan, D.G.: A recent volcanic eruption beneath the West Antarctic ice sheet, *Nature Geoscience*, 1(2),
122-125. <https://doi.org/10.1038/ngeo106>, 2008.
- Cowton, T., Nienow, P., Bartholomew, I., Sole, A. and Mair, D.: Rapid erosion beneath the Greenland ice
sheet. *Geology*, 40(4), 343-346. <https://doi.org/10.1130/G32687.1>, 2012.
- 705 Cowton, T., Nienow, P., Bartholomew, I., Sole, A. and Mair, D.: Rapid erosion beneath the Greenland ice
sheet. *Geology*, 40(4), 343-346. <https://doi.org/10.1130/G32687.1>, 2012.
- Das, S.B., Joughin, I., Behn, M.D., Howat, I.M., King, M.A., Lizarralde, D. and Bhatia, M.P.: Fracture propagation to
the base of the Greenland Ice Sheet during supraglacial lake drainage. *Science*, 320(5877), 778-781.
<https://doi.org/10.1126/science.1153360>, 2008.
- 710 Das, S.B., Joughin, I., Behn, M.D., Howat, I.M., King, M.A., Lizarralde, D. and Bhatia, M.P.: Fracture propagation to
the base of the Greenland Ice Sheet during supraglacial lake drainage. *Science*, 320(5877), 778-781.
<https://doi.org/10.1126/science.1153360>, 2008.
- Davies, J. H.: Global map of solid Earth surface heat flow, *Geochemistry, Geophysics, Geosystems*, 14, 4608–4622,
<https://doi.org/10.1002/ggge.20271>, 2013.



- 715 DeConto, R.M. and Pollard, D.: A coupled climate–ice sheet modeling approach to the early Cenozoic history of the Antarctic ice sheet. *Palaeogeography, Palaeoclimatology, Palaeoecology*. 198(1), 39–52. [https://doi.org/10.1016/S0031-0182\(03\)00393-6](https://doi.org/10.1016/S0031-0182(03)00393-6), 2003.
- 720 DeConto, R.M. and Pollard, D.: Contribution of Antarctica to past and future sea-level rise. *Nature*, 531(7596), 591–597. <https://doi.org/10.1038/nature17145>, 2016.
- Denton, G.H., Prentice, M.L., Kellogg, D.E. and Kellogg, T.B.: Late Tertiary history of the Antarctic ice sheet: Evidence from the Dry Valleys. *Geology*, 12(5), 263–267. [https://doi.org/10.1130/0091-7613\(1984\)12<263:LTHOTA>2.0.CO;2](https://doi.org/10.1130/0091-7613(1984)12<263:LTHOTA>2.0.CO;2), 1984.
- 725 Denton, G.H. and Sugden, D.E.: Meltwater features that suggest Miocene ice-sheet overriding of the Transantarctic Mountains in Victoria Land, Antarctica. *Geografiska Annaler: Series A, Physical Geography*. 87(1), 67–85. <https://doi.org/10.1111/j.0435-3676.2005.00245.x>, 2005.
- 730 Domack, E., Amblàs, D., Gilbert, R., Brachfeld, S., Camerlenghi, A., Rebesco, M., Canals, M. and Urgeles, R.: Subglacial morphology and glacial evolution of the Palmer deep outlet system, Antarctic Peninsula. *Geomorphology*. 75(1), 125–142. <https://doi.org/10.1016/j.geomorph.2004.06.013>, 2006.
- 735 Dow, C. F., Werder, M. A., Babonis, G., Nowicki, S., Walker, R. T., Csatho, B., & Morlighem, M.: Dynamics of active subglacial lakes in Recovery Ice Stream. *Journal of Geophysical Research: Earth Surface*, 123, 837–850. <https://doi.org/10.1002/2017JF004409>, 2018.
- 740 Dowdeswell, J.A., Evans, J. and Ó Cofaigh, C.: Submarine landforms and shallow acoustic stratigraphy of a 400 km-long fjord-shelf-slope transect, Kangerlussuaq margin, East Greenland. *Quaternary Science Reviews*. 29(25), 3359–3369. <https://doi.org/10.1016/j.quascirev.2010.06.006>, 2010.
- 745 Dowdeswell, J.A., Canals, M., Jakobsson, M., Todd, B.J., Dowdeswell, E.K. and Hogan, K.A.: The variety and distribution of submarine glacial landforms and implications for ice-sheet reconstruction. In: Dowdeswell, J. A., Canals, M., Jakobsson, M., Todd, B. J., Dowdeswell, E. K., and Hogan, K. A. (eds) (2016). *Atlas of Submarine Glacial Landforms: Modern, Quaternary and Ancient*, Geological Society, London, *Memoirs*, 46, 519–552. <https://doi.org/10.1144/M46.183>, 2016.
- 750 Dowsett, H.J.: The PRISM palaeoclimate reconstruction and Pliocene sea-surface temperature. In: Williams, M., Haywood, A.M., Gregory, F.J. and Schmidt, D.N. (eds) (2007). *Deep-Time Perspectives on Climate Change: Marrying the Signal from Computer Models and Biological Proxies*. Geological Society of London, *Micropalaeontological Society Special Publication*, 459–480, 2007.
- Elsworth, C. W., and Suckale, J.: Rapid ice flow rearrangement induced by subglacial drainage in West Antarctica, *Geophysical Research Letters*, 43, 11,697–11,707, <https://doi.org/10.1002/2016GL070430>, 2016.



- 755 Engelhardt, H., Humphrey, N., Kamb, B. and Fahnestock, M.: Physical conditions at the base of a fast moving Antarctic ice stream. *Science*. 248(4951), 57-59. <https://doi.org/10.1126/science.248.4951.57>, 1990.
- 760 Escutia, C., Bárcena, M.A., Lucchi, R.G., Romero, O., Ballegeer, A.M., Gonzalez, J.J. and Harwood, D.M.: Circum-Antarctic warming events between 4 and 3.5 Ma recorded in marine sediments from the Prydz Bay (ODP Leg 188) and the Antarctic Peninsula (ODP Leg 178) margins. *Global and Planetary Change*. 69(3), 170-184. <https://doi.org/10.1016/j.gloplacha.2009.09.003>, 2009.
- 765 Evatt, G.W., Fowler, A.C., Clark, C.D. and Hulton, N.R.J.: Subglacial floods beneath ice sheets, *Philosophical Transactions of the Royal Society of London A: Mathematical, Physical and Engineering Sciences*. 364(1844), 1769-1794. <https://doi.org/10.1098/rsta.2006.1798>, 2006.
- Feldmann, J. and Levermann, A.: Collapse of the West Antarctic Ice Sheet after local destabilization of the Amundsen Basin, *Proceedings of the National Academy of Sciences*, 112(46), 14191-14196. doi: 10.1073/pnas.1512482112, 2015.
- 770 Flament, T., Berthier, E. and Rémy, F.: Cascading water underneath Wilkes Land, East Antarctic ice sheet, observed using altimetry and digital elevation models. *The Cryosphere*, 8(2), 673-687. <https://doi.org/10.5194/tc-8-673-2014>, 2014.
- 775 Flowers, G.E.: Modelling water flow under glaciers and ice sheets. *Proceedings of the Royal Society A*, 471(2176). <https://doi.org/10.1098/rspa.2014.0907>, 2015.
- Fricter, H.A., Scambos, T., Bindschadler, R. and Padman, L.: An active subglacial water system in West Antarctica mapped from space. *Science*. 315(5818), 1544-1548. <https://doi.org/10.1126/science.1136897>, 2007.
- 780 Fricter, H.A. and Scambos, T.: Connected subglacial lake activity on lower Mercer and Whillans ice streams, West Antarctica, 2003–2008, *Journal of Glaciology*, 55(190), 303-315. <https://doi.org/10.3189/002214309788608813>, 2009.
- 785 Fricter, H.A., Carter, S.P., Bell, R.E. and Scambos, T.: Active lakes of Recovery Ice Stream, East Antarctica: a bedrock-controlled subglacial hydrological system. *Journal of Glaciology*, 60(223), 1015-1030. <https://doi.org/10.3189/2014JG14J063>, 2014.
- 790 Fricter, H.A., Siegfried, M.R., Carter, S.P. and Scambos, T.A.: A decade of progress in observing and modelling Antarctic subglacial water systems. *Philosophical Transactions of the Royal Society A*, 374, 20140294. <https://doi.org/10.1098/rsta.2014.0294>, 2016.
- 795 Fogwill, C.J., Turney, C.S., Meissner, K.J., Gолledge, N.R., Spence, P., Roberts, J.L., England, M.H., Jones, R.T. and Carter, L.: Testing the sensitivity of the East Antarctic Ice Sheet to Southern Ocean dynamics: past changes and future implications. *Journal of Quaternary Science*, 29(1), 91-98. <https://doi.org/10.1002/jqs.2683>, 2014.



- Fowler, A.C.: Dynamics of subglacial floods. *Proceedings of the Royal Society of London A: Mathematical, Physical and Engineering Sciences* 465 (2106), 1809-1828. <https://doi.org/10.1098/rspa.2008.0488>, 2009.
- 800 Fretwell, P., Pritchard, H.D., Vaughan, D.G., Bamber, J.L., Barrand, N.E., Bell, R., Bianchi, C., Bingham, R.G., Blankenship, D.D., Casassa, G. and Catania, G.: Bedmap2: improved ice bed, surface and thickness datasets for Antarctica. *The Cryosphere*. 7(1), 375-393. <https://doi.org/10.5194/tc-7-375-2013>, 2013.
- 805 Gales, J.A., Larter, R.D., Mitchell, N.C. and Dowdeswell, J.A.: Geomorphic signature of Antarctic submarine gullies: implications for continental slope processes. *Marine Geology*, 337, 112-124. <https://doi.org/10.1016/j.margeo.2013.02.003>, 2013.
- Golledge, N.R., Fogwill, C.J., Mackintosh, A.N. and Buckley, K.M.: Dynamics of the last glacial maximum Antarctic ice-sheet and its response to ocean forcing, *Proceedings of the National Academy of Sciences*. <https://doi.org/10.1073/pnas.1205385109>, 2012.
- 810 Golledge, N.R., Levy, R.H., McKay, R.M., Fogwill, C.J., White, D.A., Graham, A.G., Smith, J.A., Hillenbrand, C.D., Licht, K.J., Denton, G.H. and Ackert, R.P.: Glaciology and geological signature of the Last Glacial Maximum Antarctic ice sheet. *Quaternary Science Reviews*. 78, 225-247. <https://doi.org/10.1016/j.quascirev.2013.08.011>, 2013.
- 815 Golledge, N.R., Menviel, L., Carter, L., Fogwill, C.J., England, M.H., Cortese, G. and Levy, R.H.: Antarctic contribution to meltwater pulse 1A from reduced Southern Ocean overturning, *Nature communications*, 5, 5107. <https://doi.org/10.1038/ncomms6107>, 2014.
- 820 Graham, A. G. C., Larter, R.D., Gohl, K., Hillenbrand, C.-D., Smith, J.A. and Kuhn, G.: Bed form signature of a West Antarctic ice stream reveals a multitemporal record of flow and substrate control, *Quaternary Science Reviews*, 28, 2774-2793, <https://doi.org/10.1016/j.quascirev.2009.07.003>, 2009.
- 825 Graham, A.G., Larter, R.D., Gohl, K., Dowdeswell, J.A., Hillenbrand, C.D., Smith, J.A., Evans, J., Kuhn, G. and Deen, T.: Flow and retreat of the Late Quaternary Pine Island-Thwaites palaeo-ice stream, West Antarctica, *Journal of Geophysical Research: Earth Surface*, 115(F3). <https://doi.org/10.1029/2009JF001482>, 2010.
- 830 Gray, L., Joughin, I., Tulaczyk, S., Spikes, V.B., Bindschadler, R. and Jezek, K.: Evidence for subglacial water transport in the West Antarctic Ice Sheet through three-dimensional satellite radar interferometry, *Geophysical Research Letters*, 32(3), <https://doi.org/10.1029/2004GL021387>, 2005.
- 835 Greenwood, S.L., Clark, C.D. and Hughes, A.L.: Formalising an inversion methodology for reconstructing ice-sheet retreat patterns from meltwater channels: application to the British Ice Sheet. *Journal of Quaternary Science*. 22(6), 637-645. <https://doi.org/10.1002/jqs.1083>, 2007.
- Greenwood, S.L., Clason, C.C. and Jakobsson, M.: Ice-flow and meltwater landform assemblages in the Gulf of Bothnia. In: Dowdeswell, J. A., Canals, M., Jakobsson, M., Todd, B. J., Dowdeswell, E. K., and Hogan, K. A.



- (eds) (2016). Atlas of Submarine Glacial landforms: Modern, Quaternary and Ancient, Geological Society, London, Memoirs, 46, 321-324. <https://doi.org/10.1144/M46.163>, 2016.
- 840
- Greenwood, S.L., Clason, C.C., Nyberg, J., Jakobsson, M. and Holmlund, P.: The Bothnian Sea ice stream: early Holocene retreat dynamics of the south-central Fennoscandian Ice Sheet. *Boreas* 46, 346-362. <https://doi.org/10.1111/bor.12217>, 2017.
- 845
- Hanna, E., Huybrechts, P., Steffen, K., Cappelen, J., Huff, R., Shuman, C., Irvine-Fynn, T., Wise, S. and Griffiths, M.: Increased runoff from melt from the Greenland Ice Sheet: a response to global warming. *Journal of Climate*, 21(2), 331-341. <https://doi.org/10.1175/2007JCLI1964.1>, 2008.
- Holtedahl, O.: Notes on the formation of fjords and fjord valleys, *Geografiska Annaler*, 49A: 199–203, <https://doi.org/10.1080/04353676.1967.11879749>, 1967.
- 850
- Humbert, A., Steinhage, D., Helm, V., Beyer, S. and Kleiner, T.: Missing evidence of widespread subglacial lakes at Recovery Glacier, Antarctica. *Journal of Geophysical Research: Earth Surface*, 123. <https://doi.org/10.1029/2017JF004591>, 2018.
- 855
- Ives, J.D.: Glacial drainage channels as indicators of lateglacial conditions in Labrador-Ungava: a discussion. *Cahiers de Géographie Quebec*, 5. 57–72, <https://doi.org/10.7202/020113ar>, 1958.
- Jansen, J.D., Codilean, A.T., Stroeven, A.P., Fabel, D., Hättstrand, C., Kleman, J., Harbor, J.M., Heyman, J., Kubik, P.W. and Xu, S.: Inner gorges cut by subglacial meltwater during Fennoscandian ice sheet decay. *Nature communications*, 5, 3815. <https://doi.org/10.1038/ncomms4815>, 2014.
- 860
- Jordan, T.A., Ferraccioli, F., Corr, H., Graham, A., Armadillo, E. and Bozzo, E.: Hypothesis for mega-outburst flooding from a palaeo-subglacial lake beneath the East Antarctic Ice Sheet. *Terra Nova*, 22. 283-289. <https://doi.org/10.1111/j.1365-3121.2010.00944.x>, 2010.
- 865
- Joughin, I., Tulaczyk, S., Bindschadler, R. and Price, S.F.: Changes in West Antarctic ice stream velocities: observation and analysis. *Journal of Geophysical Research: Solid Earth*, 107(B11). <https://doi.org/10.1029/2001JB001029>, 2002.
- 870
- Joughin, I., Tulaczyk, S., Bamber, J.L., Blankenship, D., Holt, J.W., Scambos, T. and Vaughan, D.G.: Basal conditions for Pine Island and Thwaites Glaciers, West Antarctica, determined using satellite and airborne data. *Journal of Glaciology*, 55(190), 245-257. <https://doi.org/10.3189/002214309788608705>, 2009.
- 875
- Joughin, I., Smith, B.E. and Medley, B.: Marine ice sheet collapse potentially under way for the Thwaites Glacier Basin, West Antarctica, *Science*, 344(6185), 735-738. <https://doi.org/10.1126/science.1249055>, 2014.



- 880 Kamb, B. (2001). Basal zone of the West Antarctic ice streams and its role in lubrication of their rapid motion. In: Alley, R.B. and Bindschadler, R.A. (Eds): The West Antarctic ice sheet: behavior and environment. American Geophysical Union, 157-199. <https://doi.org/10.1029/AR077p0157>, 2001.
- King, J. C. and Turner, J.: Antarctic meteorology and climatology, Cambridge University Press, 2007.
- 885 Kingslake, J., Ely, J.C., Das, I. and Bell, R.E.: Widespread movement of meltwater onto and across Antarctic ice shelves. *Nature*, 544. 349-352, <https://doi.org/10.1038/nature22049>, 2017.
- Kuhn, G., Hillenbrand, C.D., Kasten, S., Smith, J.A., Nitsche, F.O., Frederichs, T., Wiers, S., Ehrmann, W., Klages, J.P. and Mogollón, J.M.: Evidence for a palaeo-subglacial lake on the Antarctic continental shelf, *Nature Communications*, 8, 15591. <https://doi.org/10.1038/ncomms15591>, 2017.
- 890 LaMasurier, W.: Shield volcanoes of Marie Byrd Land, West Antarctic rift: oceanic island similarities, continental signature, and tectonic controls. *Bulletin of Volcanology*, 75. 726-744, <https://doi.org/10.1007/s00445-013-0726-1>, 2013.
- 895 Larter, R.D., Graham, A.G., Gohl, K., Kuhn, G., Hillenbrand, C.D., Smith, J.A., Deen, T.J., Livermore, R.A. and Schenke, H.W.: Subglacial bedforms reveal complex basal regime in a zone of paleo-ice stream convergence, Amundsen Sea embayment, West Antarctica. *Geology*, 37(5), 411-414. <https://doi.org/10.1130/G25505A.1>, 2009.
- 900 Lewis, A.R., Marchant, D.R., Kowalewski, D.E., Baldwin, S.L. and Webb, L.E.: The age and origin of the Labyrinth, western Dry Valleys, Antarctica: Evidence for extensive middle Miocene subglacial floods and freshwater discharge to the Southern Ocean. *Geology*. 34(7), 513-516. <https://doi.org/10.1130/G22145.1>, 2006.
- 905 Lewis, A.R., Marchant, D.R., Ashworth, A.C., Hemming, S.R. and Machlus, M.L.: Major middle Miocene global climate change: Evidence from East Antarctica and the Transantarctic Mountains. *Geological Society of America Bulletin*. 119(11-12), 1449-1461. <https://doi.org/10.1130/B26134>, 2007.
- 910 Lewis, A.R., Marchant, D.R., Ashworth, A.C., Hedenäs, L., Hemming, S.R., Johnson, J.V., Leng, M.J., Machlus, M.L., Newton, A.E., Raine, J.I. and Willenbring, J.K.: Mid-Miocene cooling and the extinction of tundra in continental Antarctica. *Proceedings of the National Academy of Sciences*. 105(31), 10676-10680. <https://doi.org/10.1073/pnas.0802501105>, 2008.
- 915 Livingstone, S. J., Clark, C. D., and Tarasov, L.: Modelling North American palaeo-subglacial lakes and their meltwater drainage pathways. *Earth and Planetary Science Letters*, 375. 13–33, <https://doi.org/10.1016/j.epsl.2013.04.017>, 2013a.
- Livingstone, S., Clark, C., Woodward, J. and Kingslake, J.: Potential subglacial lake locations and meltwater drainage pathways beneath the Antarctic and Greenland ice sheets. *The Cryosphere*, 7(6), 1721-1740. <https://doi.org/10.5194/tc-7-1721-2013>, 2013b.



- 920 Livingstone, S.J., Utting, D.J., Ruffell, A., Clark, C.D., Pawley, S., Atkinson, N. and Fowler, A.C.: Discovery of relict subglacial lakes and their geometry and mechanism of drainage. *Nature Communications*, 7:11767. <https://doi.org/10.1038/ncomms11767>, 2016.
- 925 Loose, B., Naveira Garabato, A.C., Schlosser, P., Jenkins, W.J., Vaughan, D. and Heywood, K.J.: Evidence of an active volcanic heat beneath the Pine Island Glacier, *Nature Communications*, 9:2431. <https://doi.org/10.1038/s41467-018-04421-3>, 2018.
- 930 Lowe, A.L. and Anderson, J.B.: Reconstruction of the West Antarctic ice sheet in Pine Island Bay during the Last Glacial Maximum and its subsequent retreat history. *Quaternary Science Reviews*, 21(16-17), 1879-1897. [https://doi.org/10.1016/S0277-3791\(02\)00006-9](https://doi.org/10.1016/S0277-3791(02)00006-9), 2002.
- Lowe, A.L. and Anderson, J.B.: Evidence for abundant subglacial meltwater beneath the paleo-ice sheet in Pine Island Bay, Antarctica. *Journal of Glaciology*, 49(164), 125-138. <https://doi.org/10.3189/172756503781830971>, 2003.
- 935 Mannerfelt, C.M.: Några glacialmorfologiska Formelement, *Geografiska Annaler*, 27. 1–239, 1945.
- Marchant, D.R., Denton, G.H., Sugden, D.E. and Swisher III, C.C.: Miocene glacial stratigraphy and landscape evolution of the western Asgard Range, Antarctica. *Geografiska Annaler: Series A, Physical Geography*, 75(4), 303-330. <https://doi.org/10.1080/04353676.1993.11880398>, 1993.
- 940 Marchant, D.R. and Denton, G.H.: Miocene and Pliocene paleoclimate of the Dry Valleys region, southern Victoria Land: a geomorphological approach. *Marine Micropaleontology*, 27(1-4), 253-271. [https://doi.org/10.1016/0377-8398\(95\)00065-8](https://doi.org/10.1016/0377-8398(95)00065-8), 1996.
- 945 Marchant, D.R., Jamieson, S.S. and Sugden, D.E.: The geomorphic signature of massive subglacial floods in Victoria Land, Antarctica. *Geophysical Monograph*, 192, 111-126. <https://doi.org/10.1029/2010GM000943>, 2011.
- Martos, Y.M., Catalán, M., Jordan, T.A., Golynsky, A., Golynsky, D., Eagles, G. and Vaughan, D.G.: Heat flux distribution of Antarctica unveiled. *Geophysical Research Letters*, 44(22), pp.11417-11426. <https://doi.org/10.1002/2017GL075609>, 2017.
- 950 Mayer, L.A., Paton, M., Gee, L., Gardner, S.V. and Ware, C.: Interactive 3-D Visualization: A tool for seafloor navigation, exploration and engineering. In *OCEANS 2000 MTS/IEEE Conference and Exhibition (Vol. 2, 913-919)*, IEEE. <https://doi.org/10.1109/OCEANS.2000.881373>, 2000.
- 955 Meyer, C.R., Fernandes, M.C., Creyts, T.T. and Rice, J.R.: Effects of ice deformation on Røthlisberger channels and implications for transitions in subglacial hydrology, *Journal of Glaciology*, 62(234), 750-762. <https://doi.org/10.1017/jog.2016.65>, 2016.

960



- Millan, R., Rignot, E., Bernier, V. and Morlighem, M.: Bathymetry of the Amundsen Sea Embayment sector of West Antarctica from operation IceBridge gravity and other data. *Geophysical Research Letters*, 44. 1360–1368, <https://doi.org/10.1002/2016GL072071>, 2017.
- 965 Miller, K.G., Wright, J.D., Browning, J.V., Kulpecz, A., Kominz, M., Naish, T.R., Cramer, B.S., Rosenthal, Y., Peltier, W.R. and Sostdian, S.: High tide of the warm Pliocene: Implications of global sea level for Antarctic deglaciation. *Geology*. 40(5), 407-410. <https://doi.org/10.1130/G32869.1>, 2012.
- Morlighem, M., Rignot, E.J., Binder, T., Blankenship, D.D., Drews, R., Eagles, G., Eisen, O., Fretwell, P., Helm, V., Hofstede, C.M., Humbert, A., Jokat, W., Karlsson, N.A., Lee, W.S., Millan, R., Mouginot, J., Paden, J.D., Rosier, S.H.R., Ruppel, A.S., Seroussi, H.L., Smith, E.C., Steinhage, D. and Young D.A.: BedMachine Antarctica v1: a new subglacial bed topography and ocean bathymetry dataset of Antarctica combining mass conservation, gravity inversion and streamline diffusion. American Geophysical Union, Fall Meeting 2018. Abstract #C51E-1117, 2018.
- 970
- 975 Nitsche, F.O., Gohl, K., Larter, R.D., Hillenbrand, C.D., Kuhn, G., Smith, J.A., Jacobs, S., Anderson, J.B. and Jakobsson, M.: Paleo ice flow and subglacial meltwater dynamics in Pine Island Bay, West Antarctica. *The Cryosphere*. 7(1), 249-262. <https://doi.org/10.5194/tc-7-249-2013>, 2013.
- Noormets, R., Dowdeswell, J.A., Larter, R.D., Ó Cofaigh, C. and Evans, J.: Morphology of the upper continental slope in the Bellingshausen and Amundsen Seas—Implications for sedimentary processes at the shelf edge of West Antarctica. *Marine Geology*. 258(1), 100-114. <https://doi.org/10.1016/j.margeo.2008.11.011>, 2009.
- 980
- Nye, J.F.: Water flow in glaciers: jökulhlaups, tunnels and veins. *Journal of Glaciology*, 17 (76), 181–207, <https://doi.org/10.3189/S0022143000001354X>, 1976.
- 985
- Ó Cofaigh, C., Pudsey, C.J., Dowdeswell, J.A. and Morris, P.: Evolution of subglacial bedforms along a paleo-ice stream, Antarctic Peninsula continental shelf. *Geophysical Research Letters*, 29(8). <https://doi.org/10.1029/2001GL014488>, 2002.
- 990
- Ó Cofaigh, C., Dowdeswell, J.A., Allen, C.S., Hiemstra, J.F., Pudsey, C.J., Evans, J. and Evans, D.J.: Flow dynamics and till genesis associated with a marine-based Antarctic palaeo-ice stream. *Quaternary Science Reviews*, 24(5-6), 709-740. <https://doi.org/10.1016/j.quascirev.2004.10.006>, 2005.
- O'Connor, J.E. and Baker, V.R.: Magnitudes and implications of peak discharges from glacial Lake Missoula. *Geological Society of America Bulletin*, 104. 267–279, [https://doi.org/10.1130/0016-7606\(1992\)104<0267:MAIOPD>2.3.CO;2](https://doi.org/10.1130/0016-7606(1992)104<0267:MAIOPD>2.3.CO;2), 1992.
- 995
- Oswald, G.K.A. and Robin, G.D.Q.: Lakes beneath the Antarctic ice sheet. *Nature*. 245, 251-254. <https://doi.org/10.1038/245251a0>, 1973.
- 1000
- Pattyn, F. and Van Huele, W.: Power law or power flaw?. *Earth Surface Processes and Landforms*. 23(8), 761-767. [https://doi.org/10.1002/\(SICI\)1096-9837\(199808\)23\(8\)<761::AID-EPS761>3.0.CO;2-1](https://doi.org/10.1002/(SICI)1096-9837(199808)23(8)<761::AID-EPS761>3.0.CO;2-1), 1998.



- 1005 Perol, T., Rice, J. R., Platt, J. D. and Suckale, J.: Subglacial hydrology and ice stream margin locations, *Journal of Geophysical Research: Earth Surface*, 120, 1352–1368, <https://doi.org/10.1002/2015JF003542>, 2015.
- Peters, N.J., Willis, I.C. and Arnold, N.S.: Numerical analysis of rapid water transfer beneath Antarctica, *Journal of Glaciology*, 55(192), 640-650, <https://doi.org/10.3189/002214309789470923>, 2009.
- 1010 Pollard, D. and DeConto, R.M.: Modelling West Antarctic ice sheet growth and collapse through the past five million years. *Nature*. 458(7236), 329-332. <https://doi.org/10.1038/nature07809>, 2009.
- Raymo, M.E., Lisiecki, L.E. and Nisancioglu, K.H.: Plio-Pleistocene ice volume, Antarctic climate, and the global $\delta^{18}\text{O}$ record. *Science*. 313(5786), 492-495. <https://doi.org/10.1126/science.1123296>, 2006.
- 1015 Rignot, E., Bamber, J.L., Van Den Broeke, M.R., Davis, C., Li, Y., Van De Berg, W.J. and Van Meijgaard, E.: Recent Antarctic ice mass loss from radar interferometry and regional climate modelling, *Nature geoscience*, 1(2), 106-110. <https://doi.org/10.1038/ngeo102>, 2008.
- 1020 Rignot, E., Mouginot, J., Morlighem, M., Seroussi, H. and Scheuchl, B.: Widespread, rapid grounding line retreat of Pine Island, Thwaites, Smith, and Kohler glaciers, West Antarctica, from 1992 to 2011, *Geophysical Research Letters*, 41(10), 3502-3509. <https://doi.org/10.1002/2014GL060140>, 2014.
- 1025 Roberts, M.J.: Jökulhlaups: a reassessment of floodwater flow through glaciers. *Reviews of Geophysics*, 43(1). <https://doi.org/10.1029/2003RG000147>, 2005.
- Robin, G.D.Q., Swithinbank, C.W.M. and Smith, B.M.E.: Radio echo exploration of the Antarctic ice sheet, International symposium on Antarctic glaciological exploration (ISAGE), Hanover, New Hampshire, USA, 3–7 September, 1970.
- 1030 Rose, K.C., Ross, N., Bingham, R.G., Corr, H.F., Ferraccioli, F., Jordan, T.A., Le Brocq, A.M., Rippin, D.M. and Siegert, M.J.: A temperate former West Antarctic ice sheet suggested by an extensive zone of subglacial meltwater channels. *Geology*. 42(11), 971-974. <https://doi.org/10.1130/G35980.1>, 2014.
- 1035 Röthlisberger, H.: Water pressure in intra-and subglacial channels. *Journal of Glaciology*, 11(62), 177-203. <https://doi.org/10.3189/S0022143000022188>, 1972.
- 1040 Russell, A.J., Gregory, A.R., Large, A.R.G., Fleisher, P.J. and Harris, T.D.: Tunnel channel formation during the November 1996 jökulhlaup, Skeiðarárjökull, Iceland. *Annals of Glaciology*, 45. 95-103, <https://doi.org/10.3189/172756407782282552>, 2007.
- Sawagaki, T. and Hirakawa, K.: Erosion of bedrock by subglacial meltwater, Soya Coast, East Antarctica. *Geografiska Annaler: Series A, Physical Geography*. 79(4), 223-238. <https://doi.org/10.1111/1468-0459.00019>, 1997.



- 1045 Schenk, T., Csathó, B., Ahn, Y., Yoon, T., Shin, S.W. and Huh, K.I.: DEM generation from the Antarctic LiDAR data: Site report. US Geological Survey, 2004.
- Schoof, C. (2010), Ice-sheet acceleration driven by melt supply variability. *Nature*, 468(7325), 803-806.
<https://doi.org/10.1038/nature09618>, 2010.
- 1050 Schroeder, D.M., Blankenship, D.D. and Young, D.A.: Evidence for a water system transition beneath Thwaites Glacier, West Antarctica. *Proceedings of the National Academy of Sciences*, 110(30), 12225-12228.
<https://doi.org/10.1073/pnas.1302828110>, 2013.
- 1055 Selby, M.J. and Wilson, A.T.: The origin of the labyrinth, Wright Valley, Antarctica. *Geological Society of America Bulletin*, 82(2), 471-476. [https://doi.org/10.1130/0016-7606\(1971\)82\[471:TOOTLW\]2.0.CO;2](https://doi.org/10.1130/0016-7606(1971)82[471:TOOTLW]2.0.CO;2), 1971.
- Shackleton, C., Patton, H., Hubbard, A., Winsborrow, M., Kingslake, J., Esteves, M., Andreassen, K. and Greenwood, S.L.: Subglacial water storage and drainage beneath the Fennoscandian and Barents Sea ice sheets, Quaternary
1060 *Science Reviews*, 201. 13-28. <https://doi.org/10.1016/j.quascirev.2018.10.007>, 2018.
- Shepherd, A., Ivins, E., Rignot, E., Smith, B., van den Broeke, M., Velicogna, I., Whitehouse, P., Briggs, K., Joughin, I., Krinner, G. and Nowicki, S.: Mass balance of the Antarctic Ice Sheet from 1992 to 2017, *Nature*, 556, 219-222. <https://doi.org/10.1038/s41586-018-0179-y>, 2018.
- 1065 Shreve, R.L.: Movement of water in glaciers. *Journal of Glaciology*. 11(62), 205-214.
<https://doi.org/10.1017/S002214300002219X>, 1972.
- Siegert, M.J., Dowdeswell, J.A., Gorman, M.R. and McIntyre, N.F.: An inventory of Antarctic sub-glacial lakes. *Antarctic
1070 Science*. 8(3), 281-286. <https://doi.org/10.1017/S0954102096000405>, 1996.
- Siegert, M.J., Hindmarsh, R., Corr, H., Smith, A., Woodward, J., King, E.C., Payne, A.J. and Joughin, I.: Subglacial Lake Ellsworth: A candidate for in situ exploration in West Antarctica, *Geophysical Research Letters*, 31(23).
<https://doi.org/10.1029/2004GL021477>, 2004.
- 1075 Siegert, M.J., Carter, S., Tabacco, I., Popov, S. and Blankenship, D.D.: A revised inventory of Antarctic subglacial lakes. *Antarctic Science*. 17(03), 453-460. <https://doi.org/10.1017/S0954102005002889>, 2005.
- Siegert, M.J., Ross, N. and Le Brocq, A.M.: Recent advances in understanding Antarctic subglacial lakes and hydrology.
1080 *Philosophical Transactions of the Royal Society A*. 374 (2059). <https://doi.org/10.1098/rsta.2014.0306>, 2015.
- Simkins, L.M., Anderson, J.B., Greenwood, S.L., Gonnermann, H.M., Prothro, L.O., Halberstadt, A.R.W., Stearns, L.A., Pollard, D. and DeConto, R.M.: Anatomy of a meltwater drainage system beneath the ancestral East Antarctic ice sheet. *Nature Geoscience*, 10(9), 691-697. <https://doi.org/10.1038/NGEO3012>, 2017.
- 1085



- Sissons, J. B.: Supposed ice-dammed lakes in Britain, with particular reference to the Eddleston Valley, southern Scotland. *Geografiska Annaler*, 40, 159–187, <https://doi.org/10.1080/200114422.1958.11880929>, 1958.
- 1090 Smith, B.E., Fricker, H.A., Joughin, I.R. and Tulaczyk, S.: An inventory of active subglacial lakes in Antarctica detected by ICESat (2003–2008). *Journal of Glaciology*, 55(192), 573-595. https://doi.org/10.3189/002214309789470879_2009a.
- 1095 Smith, J.A., Hillenbrand, C.-D., Larter, R.D., Graham, A.G.C. and Kuhn, G.: The sediment infill of subglacial meltwater channels on the West Antarctic continental shelf. *Quaternary Research*, 71, 190-200. <https://doi.org/10.1016/j.yqres.2008.11.005>, 2009b.
- Smith, B.E., Gourmelen, N., Huth, A. and Joughin, I.: Connected subglacial lake drainage beneath Thwaites Glacier, West Antarctica. *The Cryosphere*, 11(1), 451-467. <https://doi.org/10.5194/tc-11-451-2017>, 2017.
- 1100 Stearns, L.A., Smith, B.E. and Hamilton, G.S.: Increased flow speed on a large East Antarctic outlet glacier caused by subglacial floods. *Nature Geoscience*. 1(12), 827-831. <https://doi.org/10.1038/ngeo356>, 2008.
- 1105 Sugden, D.E., Denton, G.H. and Marchant, D.R.: Subglacial meltwater channel systems and ice sheet overriding, Asgard Range, Antarctica. *Geografiska Annaler. Series A. Physical Geography*, 109-121. <https://doi.org/10.2307/520986>, 1991.
- 1110 Sugden, D.E., Summerfield, M.A., Denton, G.H., Wilch, T.I., McIntosh, W.C., Marchant, D.R. and Rutherford, R.H.: Landscape development in the Royal Society Range, southern Victoria Land, Antarctica: stability since the mid-Miocene. *Geomorphology*. 28(3), 181-200. [https://doi.org/10.1016/S0169-555X\(98\)00108-1](https://doi.org/10.1016/S0169-555X(98)00108-1), 1999.
- 1115 Sugden, D.E. and Denton, G.H.: Cenozoic landscape evolution of the Convoy Range to Mackay Glacier area, Transantarctic Mountains: Onshore to offshore synthesis. *Geological Society of America Bulletin*, 116. 840–857, <https://doi.org/10.1130/B25356.1>, 2004.
- 1120 Trusel, L.D., Frey, K.E., Das, S.B., Munneke, P.K. and Broeke, M.R.: Satellite-based estimates of Antarctic surface meltwater fluxes. *Geophysical Research Letters*. 40(23), 6148-6153. <https://doi.org/10.1002/2013GL058138>, 2013.
- 1125 Tulaczyk, S., Kamb, B. and Engelhardt, H.F.: Estimates of effective stress beneath a modern West Antarctic ice stream from till preconsolidation and void ratio, *Boreas*, 30(2), 101-114, <https://doi.org/10.1111/j.1502-3885.2001.tb01216.x>, 2001.
- U.S. Geological Survey: Landsat Image Mosaic of Antarctica (LIMA), U.S. Geological Survey Fact Sheet 2007–3116, 4 pp., 2007.



- van der Vegt, P., Janszen, A. and Moscarriello, A.: Tunnel valleys: current knowledge and future perspectives. Geological Society, London, Special Publications, 368, 75-97. <https://doi.org/10.1144/SP368.13>, 2012.
- 1130 Van Wyk de Vries, M., Bingham, R.G. and Hein, A.S.: A new volcanic province: an inventory of subglacial volcanoes in West Antarctica. Geological Society, London, Special Publications, 461(1), 231-248. <https://doi.org/10.1144/SP461.7>, 2017.
- Waitt, R.B.: Case for periodic, colossal jökulhlaups from Pleistocene Lake Missoula. Geological Society of America Bulletin, 96, 1271–1286, [https://doi.org/10.1130/0016-7606\(1985\)96<1271:CFPCJF>2.0.CO;2](https://doi.org/10.1130/0016-7606(1985)96<1271:CFPCJF>2.0.CO;2), 1985.
- 1135 Walder, J. S.: Hydraulics of subglacial cavities. Journal of Glaciology, 32(112), 439-445, <https://doi.org/10.3189/S002214300001216>, 1986.
- 1140 Walder, J.S. and Fowler, A.: Channelized subglacial drainage over a deformable bed. Journal of Glaciology, 40(134), 3-15. <https://doi.org/10.3189/S0022143000003750>, 1994.
- Wilch, T. I., McIntosh, W. C., and Dunbar, N. W.: Late Quaternary volcanic activity in Marie Byrd Land: Potential $^{40}\text{Ar}/^{39}\text{Ar}$ -dated time horizons in West Antarctic ice and marine cores, Geological Society of America Bulletin, 111, 1563–1580, <https://doi.org/10.1130/0016-7606, 1999>.
- 1145 Willis, I.C., Pope, E.L., Leysinger Vieli, G.J.-M., Arnold, N.S. and Long, S.: Drainage networks, lakes and water fluxes beneath the Antarctic ice sheet. Annals of Glaciology, 57, 96-108. <https://doi.org/10.1017/aog.2016.15>, 2016
- 1150 Wingham, D.J., Siegert, M.J., Shepherd, A. and Muir, A.S.: Rapid discharge connects Antarctic subglacial lakes. Nature, 440(7087), 1033-1036. <https://doi.org/10.1038/nature04660>, 2006.
- Wright Jr., H.E.: Tunnel valleys, glacier surges, and subglacial hydrology of the Superior Lobe, Minnesota. Geological Society of America Memoirs, 136, 251–276. <https://doi.org/10.1130/MEM136-p251>, 1973.
- 1155 Yu, H., Rignot, E., Seroussi, H. and Morlighem, M.: Retreat of Thwaites Glacier, West Antarctica, over the next 100 years using various ice flow models, ice shelf melt scenarios and basal friction laws, The Cryosphere, 12, 3861-3876. <https://doi.org/10.5194/tc-12-3861-2018>, 2018.
- 1160 Zwally, H.J., Abdalati, W., Herring, T., Larson, K., Saba, J. and Steffen, K.: Surface melt-induced acceleration of Greenland ice-sheet flow. Science, 297(5579), 218-222. <https://doi.org/10.1126/science.1072708>, 2002.
- 1165



Author contributions

1170 R.D.L., J.A.D. and K.A.H. conceived the study; they and F.O.N. participated in cruises to collect the data. J.D.K. analysed
the bathymetry and LIDAR data and conducted the channel measurements. Numerical modelling was conducted by
N.S.A., N.R.G., and J.D.K. J.D.K. wrote the initial manuscript with substantial contributions from K.A.H., J.A.D. and
R.D.L. All authors contributed to data interpretation and writing of the final manuscript. The authors declare no competing
interests.

Acknowledgements

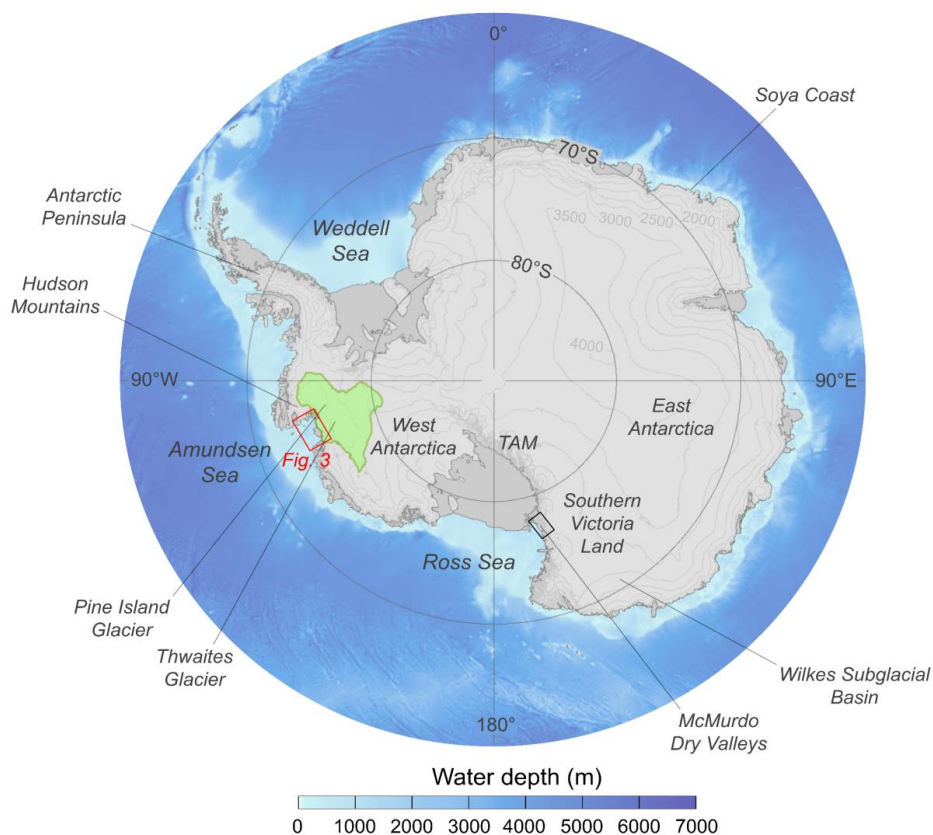
1175 We thank the masters and crews of the research vessels, RVIB Nathaniel B. Palmer (NBP), RRS James Clark Ross (JCR)
and RVIB Polarstern for their support during data acquisition. Data acquisition using the RRS James Clark Ross was
supported by funding from the UK Natural Environment Research Council's iSTAR Programme and grants
NE/J005703/1, NE/J005746/1, and NE/J005770/1. Bathymetry data from the expedition ANT-XXIII/4
(<https://doi.org/10.1594/PANGAEA.680792>) was provided courtesy of the Bathymetry Working Group, Geophysical
1180 Department, Alfred Wegener Institute, Helmholtz Centre for Polar and Marine Research. J.D.K was supported by a
Debenham Scholarship from the Scott Polar Research Institute, University of Cambridge, and a UK Natural Environment
Research Council Ph.D. studentship awarded through the Cambridge Earth System Science Doctoral Training Partnership
(grant number: NE/L002507/1). F.O.N. was supported by NSF award 0838735. K.A.H. and R.D.L. were supported by
the Natural Environment Research Council – British Antarctic Survey Polar Science for Planet Earth Programme. We
1185 thank Povl Abrahamsen for helping to initially clean the iSTAR bathymetry data.

Data availability

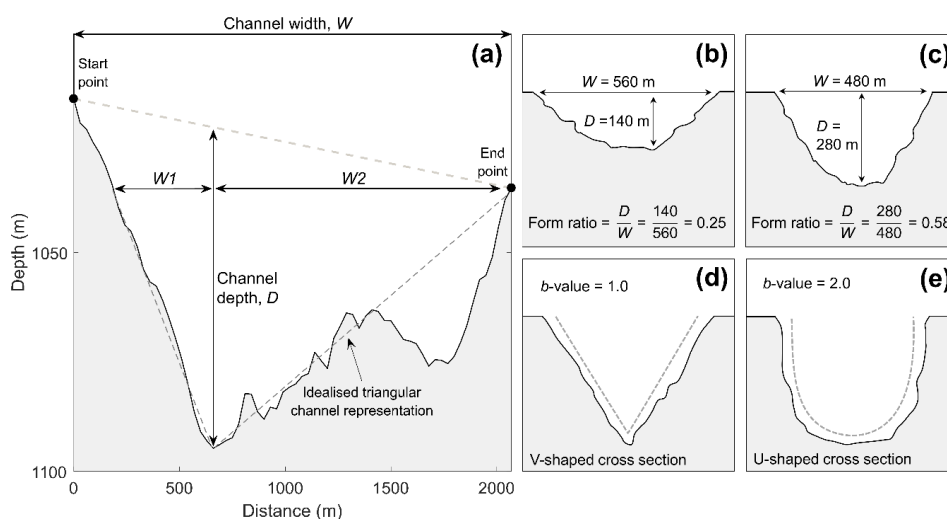
Marine geophysical data are available on request from the UK Polar Data Centre (<https://www.bas.ac.uk/data/uk-pdc/>)
and the National Centres for Environmental Information
(<https://www.ngdc.noaa.gov/mgg/bathymetry/multibeam.html>) for JCR and NBP data respectively, and on request via
1190 PANGAEA (<https://pangaea.de/>) for Polarstern data. The Dry Valleys LIDAR DEM is available online from the United
States Antarctic Resource Center (https://usarc.usgs.gov/lidar_dload.shtml). PISM model outputs are available from
N.R.G. upon reasonable request; hydrological model outputs and other datasets analysed during the study are available
upon reasonable request from the corresponding author.

1195

1200



1205 **Figure 1. Overview map displaying the location of features and regions referred to in the text.** The catchment drained by contemporary Pine Island and Thwaites glaciers is highlighted in green. The black box shows the portion of the Transantarctic Mountains (TAM) containing Wright Valley, the Royal Society Range, the Convoy Range and the Asgard Range, in which channel features have been observed. The area shown in Fig. 3 is displayed as a red box. Regional bathymetry and ice surface elevation is from BEDMAP 2 (Fretwell *et al.*, 2013).



1210 **Figure 2. Methods of quantifying channel morphometry.** (a) Output of the semi-automated algorithm used to derive
 channel cross-sectional metrics, after Noormets *et al.* (2009). Plots (b) and (c) illustrate the concept of channel form ratio:
 the ratio of channel depth to channel width. Wider, shallower channels will be characterised by lower form ratios. Plots
 (d) and (e) show the variation in channel *b*-value according to channel shape. V-shaped channels will exhibit a *b*-value
 of ~ 1, whilst U-shaped channels will be characterised by *b*-values of ~ 2. Vertical exaggeration in (a) is 20×.

1215

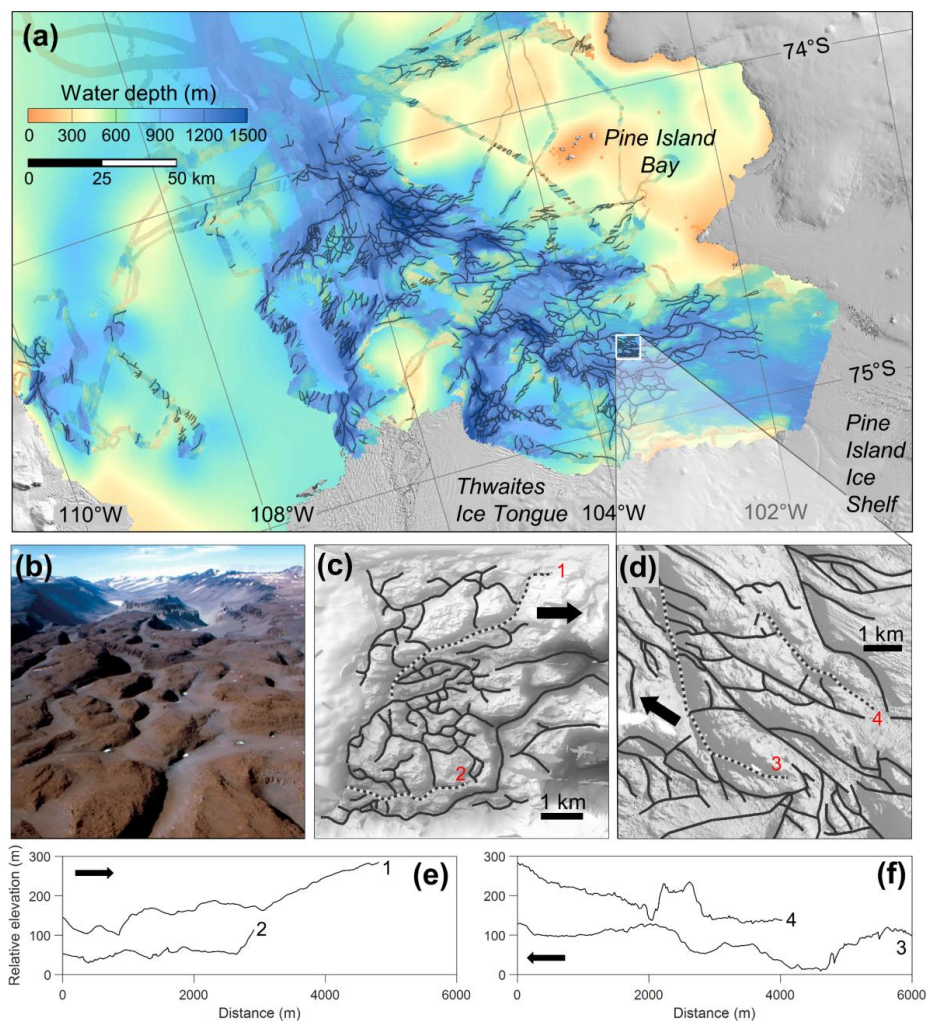
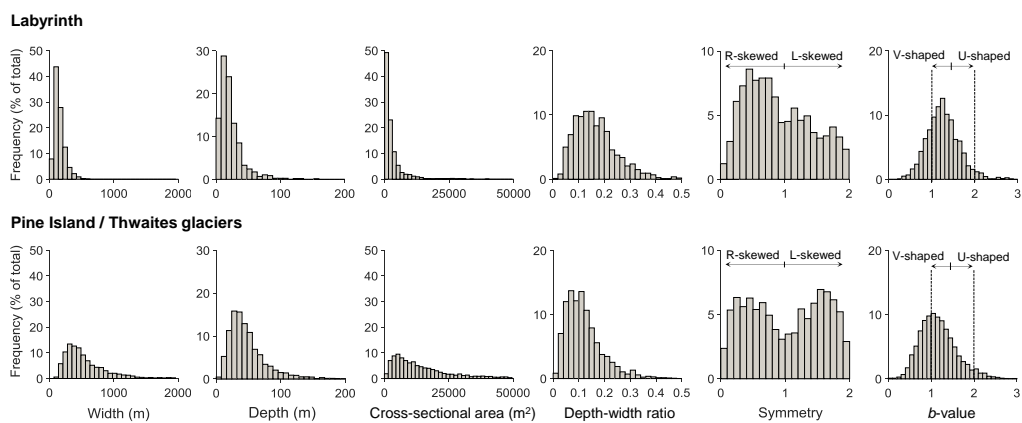
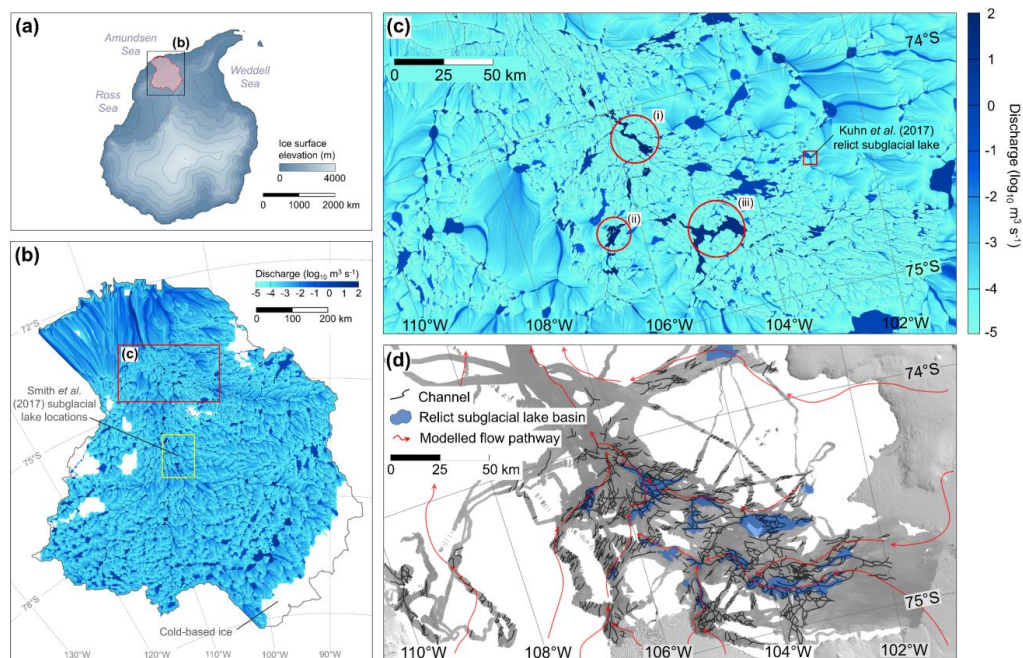


Figure 3. Channelised bathymetry of the region offshore of Pine Island and Thwaites glaciers. (a) Inner continental shelf bathymetry within Pine Island Bay, gridded at a 20 m cell size with sun illumination from the northeast. Mapped channels are displayed as black lines. Onshore topography is displayed as a shaded Landsat Image Mosaic of Antarctica (LIMA) (U.S. Geological Survey, 2007). The inset map displays the location of (a) in red and the catchment drained by contemporary Pine Island and Thwaites glaciers in green. The white square in (a) is scaled to the same dimensions as the Labyrinth, displayed in (b) and (c). (b) Oblique aerial photograph of the channel system comprising the Labyrinth (Lewis *et al.*, 2006). Channels in the foreground are ~100 m wide. (c) Digital elevation model of the Labyrinth with channels displayed as black lines. (d) Subset of the Pine Island Bay bathymetry, scaled to the same dimensions as the Labyrinth, exhibiting a series of channels. Black arrows denote the inferred direction of palaeo-ice flow. Long-profiles of the channels comprising the Labyrinth (e) and in Pine Island Bay (f) with numbers donating their locations in (c) and (d). Vertical exaggeration in (e) and (f) is 50 ×.



1230 **Figure 4. Size-frequency distributions of the morphometric characteristics of the channels comprising the Labyrinth and those present offshore of Pine Island and Thwaites glaciers.** The channels offshore of Pine Island and Thwaites glaciers from which the distributions in the lower panel are derived are displayed in Fig. 3.



1235 **Figure 5. Modelled water flow beneath Pine Island and Thwaites glaciers at the LGM.** (a) Modelled ice sheet
1236 surface at 20 ka BP (Golledge *et al.*, 2012), showing the calculated drainage catchment of Pine Island and Thwaites
1237 glaciers in red. (b) Water discharge and flow routing paths for the entire Pine Island/Thwaites catchment at the LGM,
1238 calculated at a 500 m grid resolution. The location of actively filling and draining subglacial lakes beneath the
1239 contemporary WAIS (Smith *et al.*, 2017) is outlined in yellow. Areas of cold-based ice are displayed in white. (c)
1240 Modelled subglacial water discharges within the channelised inner shelf region covered by high-resolution (90 m)
1241 swath bathymetric data. The locations of four predicted lakes, referred to as examples in the text, are shown. (d)
1242 Geomorphologically mapped channel and basin network within the high-resolution swath bathymetric data, with
1243 onshore topography from LIMA (U.S. Geological Survey, 2007). The major flow routing pathways calculated in (c)
1244 are displayed as red arrows in (d).

1245

1250

1255

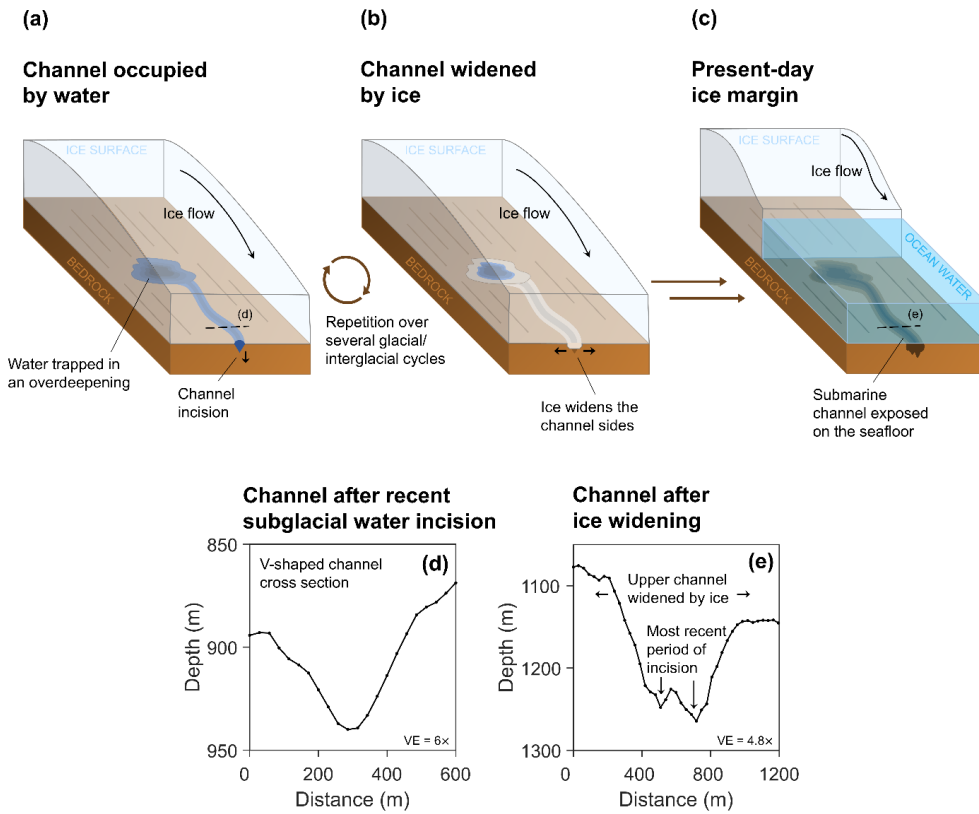


Figure 6. Schematic of channel formation over multiple glacial-interglacial cycles. (a) Channels are incised by short-lived episodes of fast-flowing subglacial meltwater, potentially released from lakes trapped in overdeepenings during ice sheet advance and retreat. (b) Repeated periods of ice overriding widens the top of the channels. (c) A composite channel feature, produced over multiple glaciations, is left exposed on the seafloor. (d) Example of a more recently incised channel, characterised by a V-shaped cross section. (e) Cross section of a channel persisting from previous glacial periods containing both V-shaped meltwater signatures and a wide upper channel section eroded by ice. Vertical exaggeration (VE) is 6× in (d) and 4.8× in (e).

1260

1265

1270



1275

Table 1. Details of the geophysical cruise data used in this investigation.

Cruise / ID	Ship	Year	Multibeam system	Principal investigator
ANT-XXIII/4	Polarstern	2006	Hydrosweep DS2	Gohl, K.
JR179	James Clark Ross	2008	EM120	Larter, R.
JR294	James Clark Ross	2014	EM122	Heywood, K.
NBP0001	N.B. Palmer	2000	SeaBeam 2112	Jacobs, S.
NBP0702	N.B. Palmer	2007	EM120	Jacobs, S.
NBP0901	N.B. Palmer	2009	EM120	Jacobs, S.
NBP1210	N.B. Palmer	2013	EM120	Halanych, K.
NBP9902	N.B. Palmer	1999	SeaBeam 2112	Anderson, J.

1280

1285

1290

1295

1300

1305



Table 2. Volume, filling time, local steady-state discharge, and potential mean flood discharge of lakes displayed in Fig. 5.

Lake	Local steady-state water discharge (m ³ s ⁻¹)	Lake volume (km ³)	Time to fill (years)	Local potential mean discharge (m ³ s ⁻¹)*	Total upstream volume (km ³)	Potential mean flood discharge** (m ³ s ⁻¹)
(i)	139	3.29	0.73	78.2	2762	65690
(ii)	101	3.47	1.09	82.5	2329	55390
(iii)	32.2	19.9	19.6	473	389	9251
(iv)***	0.23	0.33	45.1	7.8	0.58	13.8

*Local mean discharge calculated by assuming drainage of the lake in 16 months, assuming no further inflow into the basin during drainage (c.f. Wingham *et al.* 2006).

**Potential mean flood discharge calculated by assuming drainage of a large upstream lake in 16 months (c.f. Wingham *et al.* 2006) which triggers the cascading drainage of all lakes downstream from that initial event.

***Basin suggested to be a relict subglacial lake by Kuhn *et al.* (2017).